AD

RSIC-642

FUNDAMENTALS OF SELECTED ASPECTS OF DEFORMATION CHARACTERISTICS OF ADHESIVE-BONDED JOINTS AND METAL-ADHESIVE INTERFACES

by

Koichi Masubuchi
R. E. Keith

January 1967

DISTRIBUTION OF THIS DOCUMENT IS UNLIMITED

Battelle Memorial Institute
Contract No. DA-01-021-AMC-14693(Z)

REDSTONE SCIENTIFIC INFORMATION CENTER
REDSTONE ARSENAL, ALABAMA

JOINTLY SUPPORTED BY

U.S. ARMY MISSILE COMMAND

GEORGE C. MARSHALL SPACE FLIGHT CENTER

27 January 1967 RSIC-642

FUNDAMENTALS OF SELECTED ASPECTS OF DEFORMATION CHARACTERISTICS OF ADHESIVE-BONDED JOINTS AND METAL-ADHESIVE INTERFACES

by

Koichi Masubuchi
R. E. Keith

Contract No. DA-01-021-AMC-14693(Z)
Battelle Memorial Institute
Columbus Laboratories
Columbus, Ohio

DISTRIBUTION OF THIS DOCUMENT IS UNLIMITED

Research Branch
Redstone Scientific Information Center
Research and Development Directorate
U. S. Army Missile Command
Redstone Arsenal, Alabama 35809

ABSTRACT

This report presents a state-of-the-art survey on selected aspects of fundamentals of deformation characteristics of adhesive-bonded joints and metal-adhesive interfaces.

The report is divided into three separate parts:

Chapter 1: Fundamentals of deformation and Fracture of Adhesive-Bonded joints.
Chapter 2: Mechanisms of Deformation of Metal-Adhesive Interfaces.
Chapter 3: Conclusions and Recommendations.

Chapter 1 covers the following subjects:

1) Theoretical analyses of elastic stress distribution in adhesive-bonded joints.
2) Experimental stress analyses of adhesive-bonded joints.
3) Rheology of adhesive-bonded joints.
4) Fracture of adhesive-bonded joints.
5) Effects of loading and environmental conditions on deformation and fracture of adhesive-bonded joints.
6) Design and fabrication problems.

Chapter 2 discusses atomistic mechanisms of deformation of metal-adhesive interfaces.

Chapter 3 presents the conclusions derived from findings of the survey. Also, on the basis of findings observed during this survey, recommendations are given for future research for better understanding of the fundamentals of deformation and fracture of adhesive-bonded joints.

The report was written for the specific purpose of assisting another investigation in the field of adhesive-bonded joints. Therefore, it has somewhat narrow objectives. The report is not intended to be a comprehensive treatment of the subject of adhesive-bonded joints.

FOREWORD

The purpose of this survey was to review current information available on certain selected fundamentals of the deformation characteristics of adhesive-bonded joints and metal-adhesive interfaces. It was requested by the Materials Engineering and Development Branch, Research and Development Directorate, U. S. Army Missile Command, Redstone Arsenal, Alabama. The main purpose of the survey is to supply information for a project, "Study of the Onset of Permanent Deformation in Structural Bonded Joints," being conducted by Auburn University under Contract DA-01-021-AMC-12832(Z).

The report, despite its narrow objectives, is being made available in the hope that it may be useful to others in addition to those from whom it was requested, as identified above. The reader is cautioned that this report was not intended as a comprehensive treatment of the subject of deformation of adhesive-bonded joints.

PRECEDING PAGE BLANK NOT FILMED.

CONTENTS

Page

ILLUSTRATIONS

Chapter 1

FUNDAMENTALS OF DEFORMATION AND FRACTURE OF ADHESIVE-BONDED JOINTS

Section I. INTRODUCTION

Investigations at Auburn University,[1,2,3] mentioned in the Foreword, have been made primarily on lap-shear joints in aluminum-alloy sheets, 0.03 to 0.007 inch thick, bonded with organic adhesives. The emphasis in this report is placed on this type joint.

The investigators hope to reach a better understanding of the basic mechanisms of deformation in adhesive-bonded joints through a study of mechanisms of deformation of metal-adhesive interfaces. Therefore, this report is divided into three separate parts:

Chapter 1: Fundamentals of Deformation and Fracture of Adhesive-Bonded Joints.
Chapter 2: Mechanisms of Deformation of Metal-Adhesive Interfaces.
Chapter 3: Conclusions and Recommendations.

Section II. A SUMMARY OF EARLIER REVIEWS

This part of the survey provides a critical review of fundamentals of deformation and fracture of adhesive-bonded joints.

Several others have prepared reviews of problems in the area covered by this part of the report. This report is not a mere repetition of any of these reviews, but takes important points from them, combines these points with new developments, and presents a review pertinent to the Auburn project. Some of the earlier reviews are described briefly below.

Houwink and DeBruyne[4] publishied the first thorough survey on the subject. This was divided into two parts: (1) Theoretical Investigation of the Stresses in Joints, and (2) Experimental Investigation of the Stresses in Joints. A book on structural adhesives,[5] published in 1951, presented a series of lectures including fundamentals of adhesion, chemistry of adhesives, and strength of glued joints.

The "Adhesives Handbook" by Perry, et al.,[6] includes a review of the fundamentals of adhesion, rheology of polymers, statistics of fracture, and an extensive review of Goland and Reissner's paper. "Structural Adhesives for Metals and Sandwich Construction" is the report of a conference held in Dayton, Ohio, in December 1952.[7]

Ljungstrom[8] reviews various aspects of Redux bonding practice at Svenska Aeroplan Aktiebolaget (SAAB) including strength data and inspection. A book by Perry[9] on "Adhesive Bonding of Reinforced Plastics" includes chapters on "Mechanics of Adhesive Joints" and "Design of Adhesive Joints."

The field of mechanics of adhesive bonding, including practical aspects and structural applications, is reviewed in a paper by Benson.[10] A good review of current literature on stress distribution is that of Sneddon[11] in a chapter of "Adhesive." DeBruyne[12] published a collection of papers from a symposium on "The Measurement of the Strength of Adhesive and Cohesive Joints" held at the General Motors Research Laboratories in 1962.

A 1964 report of Forest Products Laboratory[13] offers a survey of literature on lap joints, including theory, adhesive properties, failure, and joint design.

Gardon[14] is preparing a review on a thermodynamic approach to the interpretation of adhesion. The thermodynamic parameters are the work of adhesion, interfacial surface energy, etc., that may be related to bonding energies, solubility parameters, and cohesive energy density.

Sections III through VIII of this chapter will cover the following subjects:

1) Theoretical analyses of elastic stress distributions in adhesive-bonded joints.
2) Experimental stress analyses of adhesive-bonded joints.
3) Rheology of adhesive-bonded joints.
4) Fracture of adhesive-bonded joints.
5) Effects of loading and environmental conditions on deformation and fracture of adhesive-bonded joints.
6) Design and fabrication problems.

Section III. THEORETICAL ANALYSES OF ELASTIC STRESS DISTRIBUTIONS IN ADHESIVE-BONDED JOINTS

Extensive use of adhesive bonding in metal structures such as airframes has been a recent development. However, in more restricted uses, bonding with adhesives such as glues is centuries old. So, although the application has changed greatly, the basic idea of adhesive bonding has been with us for many years and has been studied extensively.[9,10,15] Most of the past analyses have been made on lap joints, especially those subjected to tensile loading.

1. Lap Joints Subjected to Tensile Loading

a. Background

A lap joint is a joint between two overlapping members, as shown in Figure 1. In a lap joint, stress is distributed unevenly, with the greatest stress at the ends of the joint. There are two main reasons for this: (1) differential straining and (2) eccentric loading.[6,13]

Differential straining is shown in Figure 2.[13] When a load is applied to a lap joint, the tensile strain will vary from a maximum at one end of the joint to a minimum at the other. If the adherends are identical, distribution will be the same for both except that maximum strain will be at opposite ends of the joint. The adhesive film must absorb this differential straining. This effect has been analyzed by several researchers.

Figure 3 shows the result of eccentric loading.[13] In an unloaded lap joint, the line of force does not pass through the center of the adhesive film, but is slightly offset at the ends of the bonded area. When a load is applied, a bending moment is induced. This tends to rotate the joint until the line of action of the force passes directly through the center of the adherends. This results in further stress on the adhesive. This bending condition has not been analyzed nearly as thoroughly as differential straining, since it is much more difficult to describe mathematically.

In most metal joints bonded with organic adhesives, the adhesive is weaker than the adherends. Thus, it is important to determine stress distribution in the adhesive. The factors that affect the stress distribution in adhesive-bonded joints include:

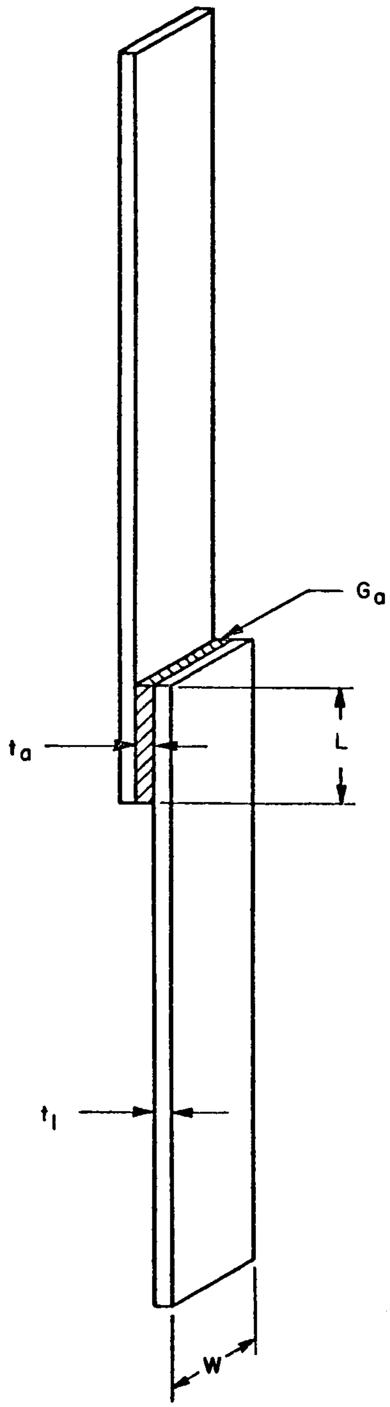

Figure 1. Typical Adhesive Bonded Lap-Type Joint[13]

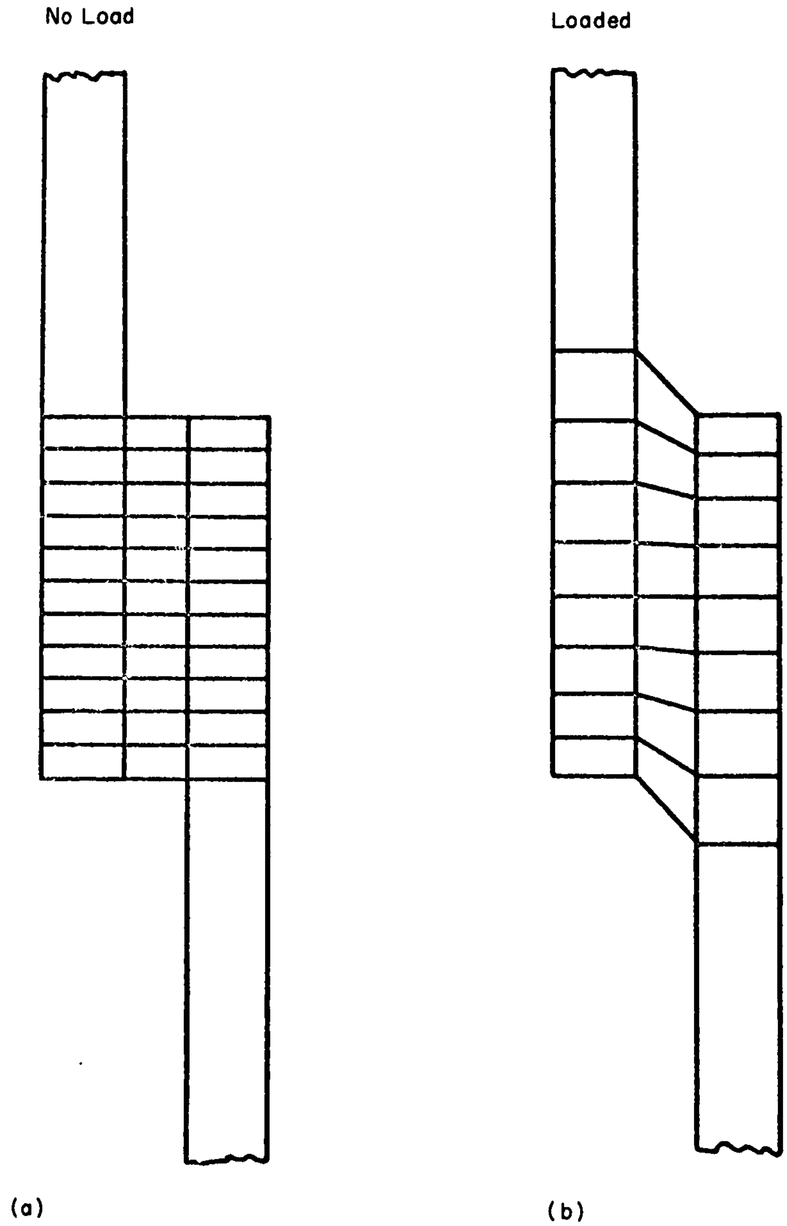

Figure 2. Differential Straining in a Lap Joint Showing the Change in a Reference Grid from: (a) Before Loading to (b) After Loading.[13]

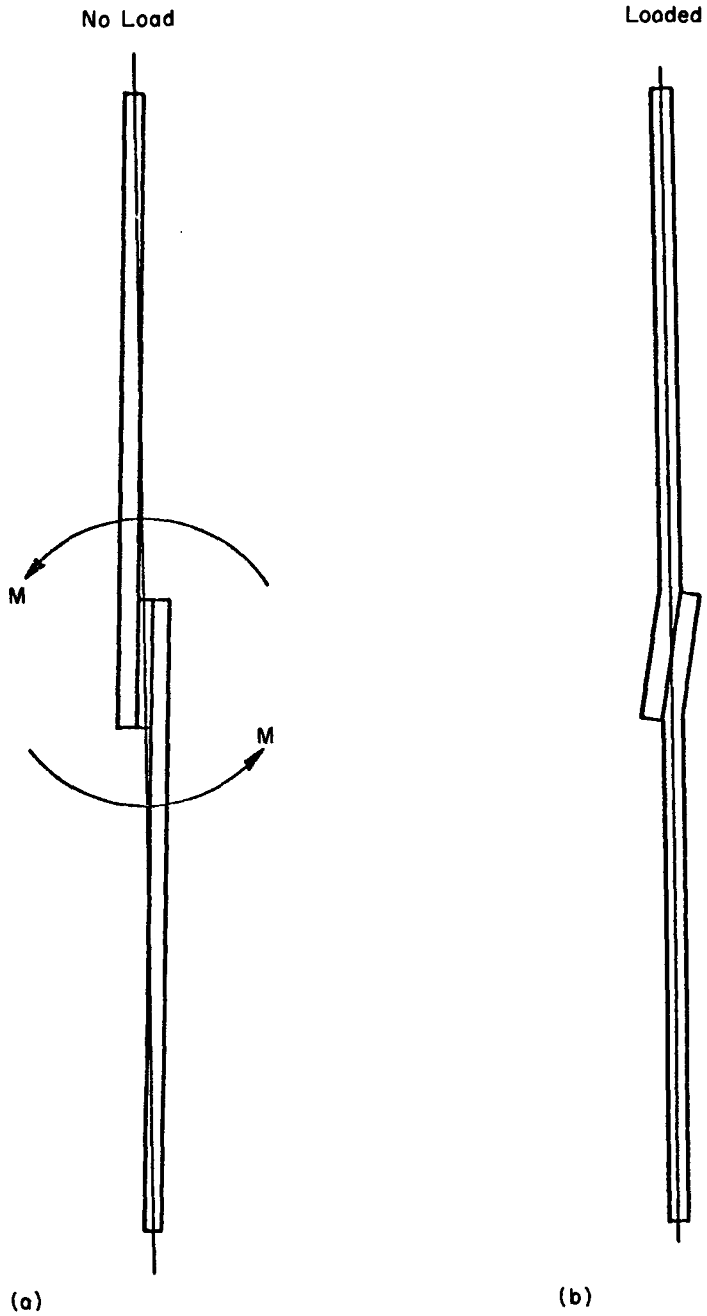

Figure 3. Bending Moment in a Lap Joint Due to Eccentric Load on the Joint Area: (a) Line of Force Through the Joint Before Loading; (b) Line of Force Through the Joint After Loading.[13]

1) Joint geometry.

   a) Length of overlap.
   b) Adhesive thickness.
   c) Adherend thickness.

2) Mechanical properties.

   a) Adhesive moduli of rigidity and of elasticity.
   b) Adherend moduli of rigidity and of elasticity.
   c) Rheological properties, fracture toughness, etc.

The theoretical analysis of stress distribution in the lap joint has been made by many investigators. Earliest papers on the subject were by Armovlevic[16] and Fillunger.[17] However, Volkersen[18] is generally credited with the first work[13] when he derived, in 1938, an analysis for rivet load distribution of multirow riveted joints in tension. The analysis is applicable to adhesive-bonded lap joints. In Volkersen's analysis, stresses due to the eccentric loading were ignored.

In 1944, Goland and Reissner[19] developed a theory which takes stresses due to the eccentric loading into account. The theory by Goland and Reissner has been modified and extended by several investigators including Plantema,[20] Sherrer,[21] and Cornell.[22] Recently, a study was made by Hahn at Douglas Aircraft Company.[23, 24]

The following paragraphs summarize some of the important work on stress distribution in lap joints under tension. This report comes primarily from an extensive review of the work edited by Eley.[25]

b. The Analysis by Volkersen

In the analysis by Volkersen,[18] it was assumed that stresses are caused solely by differential straining in the lap joint. Figure 4 illustrates the joint considered by Volkersen. Two elastic adherends of uniform thickness t_1 and t_2 and Young's moduli E_1 and E_2 were bonded by an adhesive of uniform thickness η. The adhesive was assumed to act like an elastic solid with shear modulus G_a. Maximum shear stress in the adhesive layer was found at the ends of the overlap. Volkersen defined the stress concentration, n, as the ratio of the maximum shearing stress to the mean stress and found that

$$n = \frac{\delta}{\epsilon} \left\{ \frac{2\epsilon^2 - 1 + \cosh(2\epsilon\delta)}{\sinh(2\epsilon\delta)} \right\} \qquad (1)$$

where the dimensionless quantities δ and ϵ are defined by the equations

$$\delta^2 = \frac{2c^2 G_a}{E_2 t_2 \eta} \quad , \quad \epsilon^2 = \frac{E_1 t_1 + E_2 t_2}{2E_1 t_1} \quad . \qquad (1)'$$

When the adherends are identical and of thickness t and Young's modulus E, $\epsilon^2 = 1$.

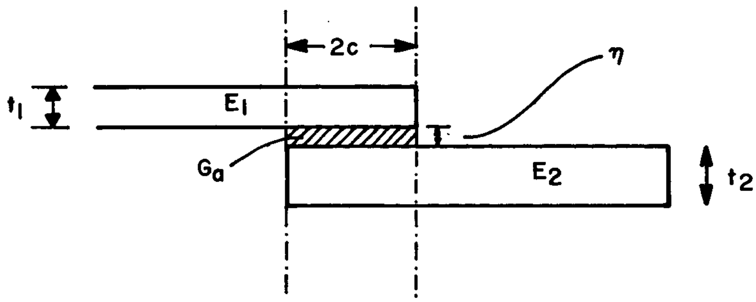

Figure 4. The Joint Considered by Volkersen.[25]

Values of the stress concentration factor n for various values of δ and ϵ are shown in Table I. The variation of these quantities is shown graphically in Figure 5.

Table I. Values of the Stress Concentration Factor n in Volkersen's Theory[25]

δ \ ε	0.5	0.7	1.0	1.5	2.0	3.0	5.0
0.4	1.132	1.106	1.053	0.5407	0.806	0.331	0.150
0.8	1.511	1.399	1.205	0.664	0.629	0.302	0.161
1.2	2.083	1.824	1.439	0.856	0.669	0.402	0.240
1.6	2.799	2.328	1.736	1.089	0.818	0.534	0.320
2.0	3.599	2.871	2.075	1.339	1.004	0.667	0.400
2.4	4.441	3.432	2.440	1.602	1.199	0.800	0.480
2.8	5.300	4.000	2.821	1.867	1.400	0.933	0.560
3.2	6.161	4.570	3.211	2.133	1.600	1.067	0.640
3.6	7.013	5.143	3.605	2.400	1.800	1.200	0.720

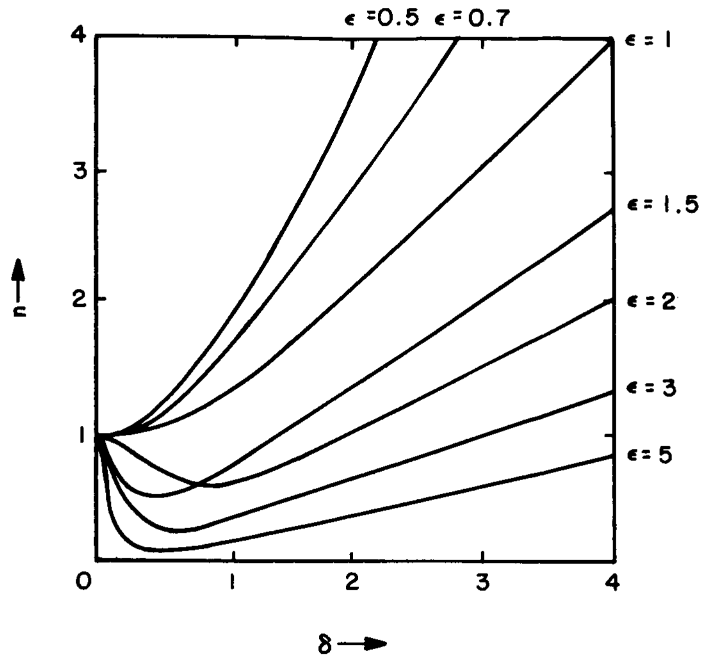

Figure 5. Variation of n with δ and ε.[25]

c. <u>The Analysis by Goland and Reissner</u>

In the analysis by Goland and Reissner,[19] stresses due to the differential straining and the eccentric loading were considered. The joint design they used is shown in Figure 6. The sheets were of equal thickness and extended an equal distance from the joint. The width of the joint was greater than the thickness of the sheets.

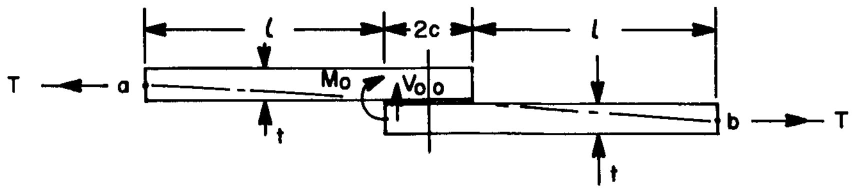

Figure 6. The Joint Considered by Goland

In conducting the analysis, the load acting on the ends of the joint was determined first, then stress distributions were determined. Goland and Reissner developed two approximate theories for determining the stress distributions. The first theory considered joints with a relatively inflexible adhesive layer. This theory generally works for analyzing joints with wooden or plastic adherends. The second theory, considering joints with a flexible adhesive layer, generally works for lap joints formed by metal sheets.

(1) Determination of the Joint End Loads. To determine the load acting on the ends of the joint, Goland and Reissner considered the lap joint and the neighboring sheet to act as a cylindrically bent plate of variable cross section and variable neutral plane. The bending moment and shearing force acting at the edge of the joint are given by Equation (2):

$$M_o = k \frac{T}{2} t$$

$$V_o = k' \cdot T \cdot \frac{t}{c} \qquad (2)$$

where
M_o = Bending moment per unit width at the end of the joint
V_o = Shearing force per unit width at the end of the joint
T = Tensile load applied to the joint
t = Thickness of the sheets
$p = \frac{T}{t}$ = Mean stress in the sheets away from the joint
E = Young's modulus of the sheet
ν = Poisson's ratio of the sheet.

The parameter k is determined by the size and properties of the adhesive as follows:

$$k = \frac{\cosh U_2 C}{\cosh U_2 C + 2 \sqrt{2} \sinh U_2 C}$$

$$k' = \sqrt[4]{6(1 - \nu^2)} \cdot \frac{c}{L} \cdot \sqrt{\frac{p}{E}} \qquad (2)'$$

where
$2C$ = Length of the joint
$U_2 = \frac{T}{D_2}$
D_2 = Flexual rigidity of the adhesive.

Values of $k = \frac{2M_o}{Tt}$ and $k' = \frac{V_o C}{Tt}$ for various values of $\frac{c}{t}\sqrt{\frac{p}{E}}$ are given in Table II. The relationship between k and $\frac{c}{t}\sqrt{\frac{p}{E}}$ also is shown in Figure 7.[19]

Table II. Values of $k = \frac{2M_o}{Tt}$ and $k' = \frac{V_o C}{Tt}$ for Various $\frac{c}{t}\sqrt{\frac{p}{E}}$

$\frac{c}{t}\sqrt{\frac{p}{E}}$	$k = \frac{2M_o}{Tt}$	$k' = \frac{V_o C}{Tt}$
0.0	1.00	0.000
0.1	0.75	0.039
0.2	0.61	0.064
0.3	0.51	0.080
0.4	0.45	0.094
0.5	0.40	0.104
0.6	0.37	0.116
0.65	0.36	0.122

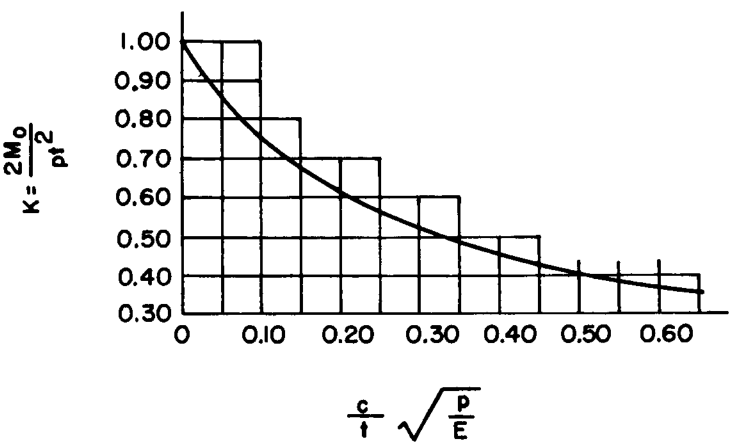

Figure 7. Plot of Moment Factor k Versus $\frac{c}{t}\sqrt{\frac{p}{E}}$

For joints of aluminum alloy with average values of overlap, and plate stresses as high as 40,000 psi, a practical lower limit for k is 0.35. This shows a considerable reduction in joint-edge moments under load from the initial value $\frac{1}{2}$ Tt. In practical cases, this reduction is as much as 65 percent. Table II also shows that only small transverse shearing forces are present at the joint edges of loaded systems with reasonable overlap. In actual joints, these shearing forces are never in excess of 0.02 T.

(2) Stress Distribution in Joints with Relatively Inflexible Adhesive Layers. Goland and Reissner assumed that where the adhesive layer in a joint is very thin it can be ignored in calculating stress distribution. Stress distributions in a very thin layer would be so small that they would have no measurable effect on stress in the joined sheets. Therefore, they considered the joint as consisting of a homogeneous slab with the same properties as the sheet material and a thickness twice that of the sheet material. The same assumption would be valid where the adhesive layer was thicker but was relatively stiff so that it had properties similar to the sheets.

Figure 8 shows a profile of such a joint including normal stress distribution at the edges. The coordinate x was defined in the direction of the joint length, with its origin at the midpoint of the joint and its positive direction to the right. In the first analysis, it was assumed that there is an even distribution of tension over the cross section of the sheet and that the moment arises from the usual elementary linear stress distribution. Any departure from this linear normal stress distribution at the joint edges would probably be at its greatest in short joints. But even with short joints, there is a remarkable degree of linearity, according to results of experiments by Tylecote.[26]

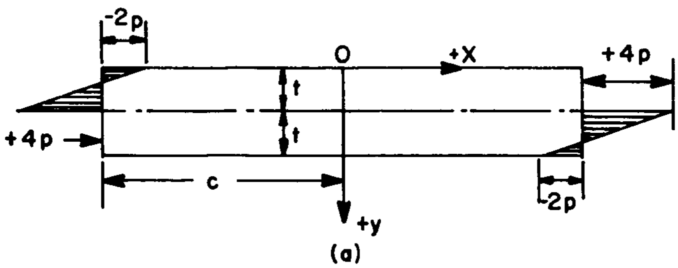

Figure 8. Diagram of Joint with Relatively Inflexible Cement Layer[19]

The following expressions show the normal stress distribution of the joint edges, with reference to Figure 8.

On $x = -c$: $\tau_{xy} = 0$,

$$\sigma_x = \begin{cases} p + pk(6y/t - 3) & (0 \leq y < t), \\ 0 & (t \leq y \leq 2t); \end{cases} \qquad (3)$$

with $p = \frac{T}{t}$;

on $x = c$: $\tau_{xy} = 0$,

$$\sigma_x = \begin{cases} 0 & (0 \leq y < t), \\ p + pk\,(9 - 6y/t) & (t \leq y \leq 2t). \end{cases} \tag{4}$$

On the remaining edges of the joint there is no normal and no shearing stress so that:

$$\text{on } y = 0,\ 2t:\ \sigma_x = \tau_{xy} = 0. \tag{5}$$

Thus, finding the stress distribution in a joint was reduced to determining the stress in a rectangular box, the box having boundary stresses on the edges, as shown in the above equations. Goland and Reissner found an approximate solution for this problem. Figure 9 was their graphic presentation of stress distribution along the midplane $y = t$ of the joint for the case in which $k = 1$. Shear stress, τ_o, normal stress in the longitudinal direction of the joint, σ_f, and tearing stress, σ_o, are shown. Figure 10 shows variations of the maximum values of these stresses as a function of k in the sheet fibers adjoining the adhesive. The existence of large stresses, particularly tearing stress in the adhesive, should be noted. This agrees with experimental observations that failure is started by the two sheets splitting apart at the joint edges on the opposite side.

(3) Stress Distribution in Joints with Relatively Flexible Adhesive Layers. Goland and Reissner considered joints with relatively flexible layers. In this case, shear strain and transverse normal strain in the sheets are small when compared to corresponding strains in the adhesive layer. The effect is that of infinitesimal springs placed between cylindrically bent plates.

The joint considered is shown in Figure 11, with loads applied to it as in the first theory. The upper and lower sheets were designated u and ℓ, respectively. Thus, bending moment in the upper sheet is denoted as M_u and in the lower sheet as M_ℓ. Similarly, vertical shear is denoted as V_u and V_ℓ and axial tension as T_u and T_ℓ.

Figure 12 shows distributions of shear stress, τ_0, and tearing stress, σ_0, in the adhesive for various dimensions of the joint. Parameters λ and β are defined as follows:

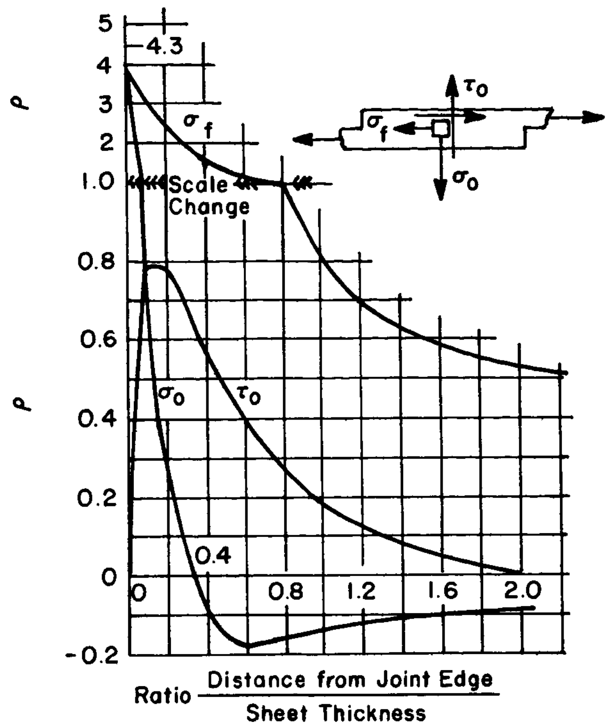

Figure 9. Stress Distribution Along Shear Plane in Joints with Relatively Inflexible Adhesive, for k = 1[19]

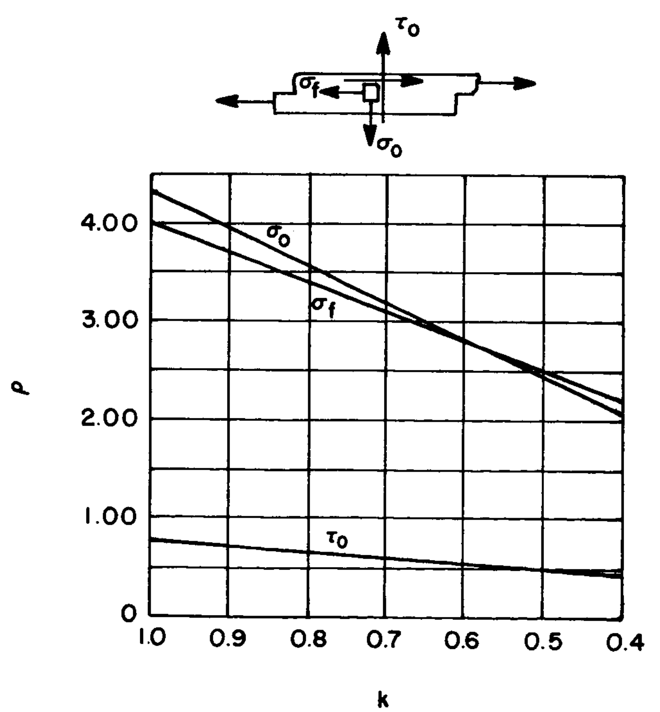

Figure 10. Maximum Stresses in Shear Plane for Joints with Relatively Adhesive Layers, Plotted Versus Moment Factor k[19]

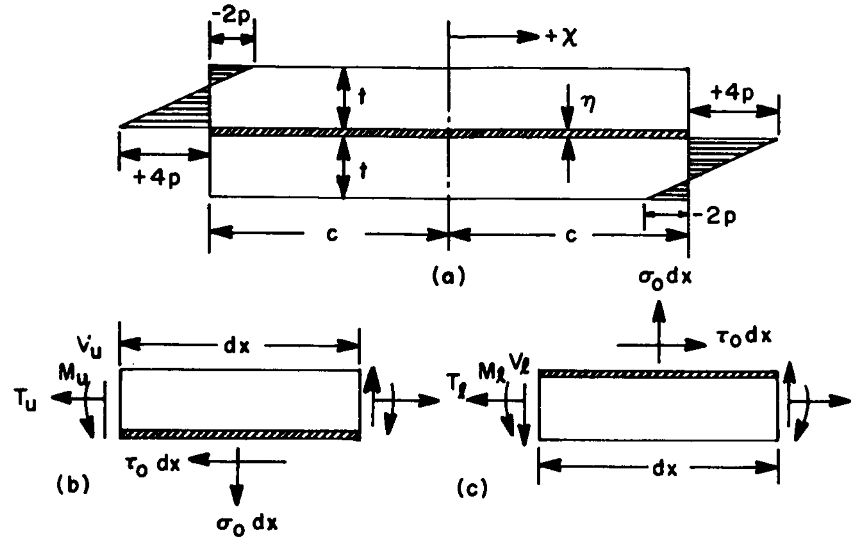

Figure 11. Diagram of Joint with Relatively Flexible Adhesive Layer;[19] (a) Profile of Joint, Showing Longitudinal Stress Distribution on Edges; (b) Element of Upper Sheet; (c) Element of Lower Sheet, for k = 1.0.

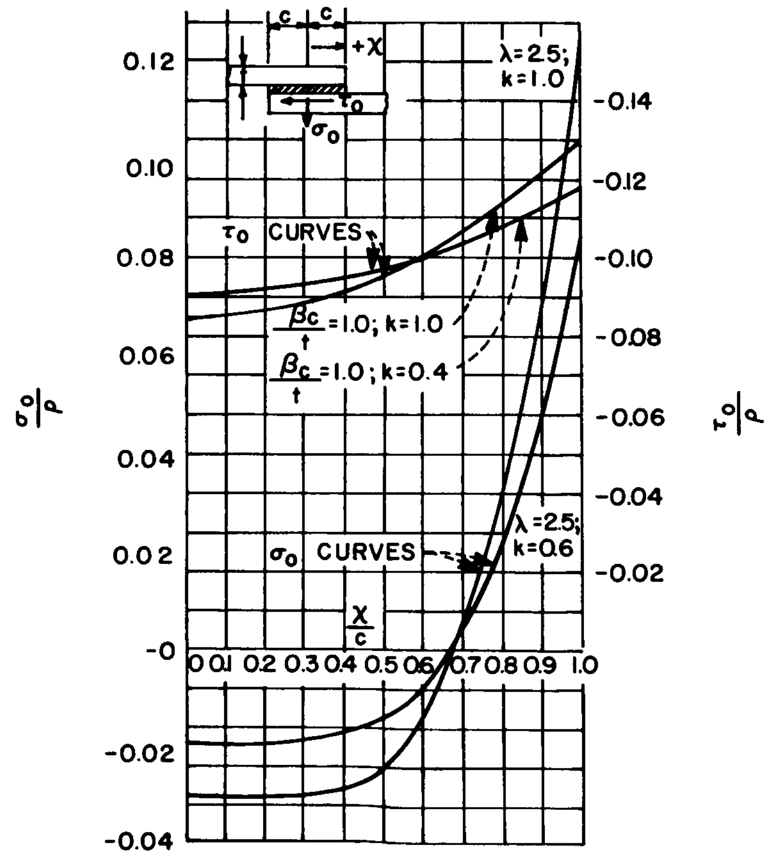

Figure 12. Stress Distribution in Adhesive in Joints with Relatively Flexible Adhesive Layers[19]

$$\lambda = \frac{c}{t} \cdot \sqrt[4]{6 \frac{E t_c}{E} \cdot \frac{t}{\eta}}$$

$$\beta = \sqrt{8 \frac{G_c}{E} \cdot \frac{t}{\eta}} \qquad (6)$$

where E_c and G_c are Young's modulus and rigidity, respectively, of the adhesive, and E is Young's modulus of the adherend. Other notations are shown in Figure 11. The definition of k is given in Equation (2)'. As shown in Figure 12, maximum stresses exist at the edge of the joint, $\frac{x}{c} = 1$.

The maximum shear stress, $(\tau_o)_{max}$, found at the edge of the joint is expressed as follows:

$$\frac{(\tau_o)_{max}}{p} \cdot \frac{c}{t} = -\frac{1}{8} \left[\frac{\beta c}{t} (1 + 3k) \coth \frac{\beta c}{t} + 3(1 - k)\right] \qquad (7)$$

Figure 13 is a plot of $\frac{(\tau_o)_{max}}{p} \cdot \frac{c}{t}$ versus $\frac{\beta c}{t}$ for various values of k. The maximum stress increases as $\frac{\beta c}{t}$ and k increase. An inspection of Equation (7) indicates that increasing the length of the joint beyond the limit $\frac{\beta c}{t} \approx 25$ has no effect on the magnitude of the maximum shear, which remains

$$(\tau_o)_{max} = -\frac{p}{8} (1 + 3k) \sqrt{8 \frac{G_c}{E} \cdot \frac{t}{\eta}} \quad .$$

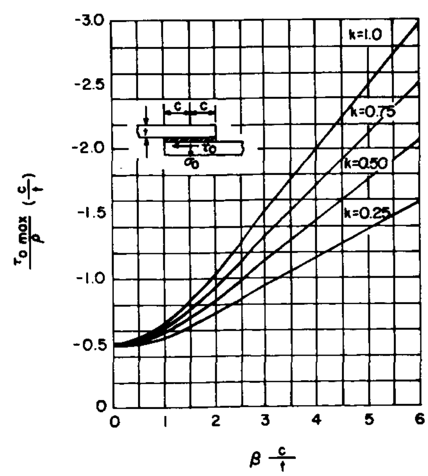

Figure 13. Maximum Shear Stress in Adhesive in Joints with Relatively Flexible Adhesive Layers[19]

The maximum value of σ_o acts at the joint edges and is given by

$$\frac{(\sigma_o)_{max}}{p}\left(\frac{c}{t}\right)^2 = \lambda^2 \; \frac{k}{2} \; \frac{\sinh 2\lambda - \sin 2\lambda}{\sinh 2\lambda + \sin 2\lambda} + \lambda k' \frac{\cosh 2\lambda + \cos 2\lambda}{\sinh 2\lambda + \sin 2\lambda}, \qquad (9)$$

for long joints, defined by λ greater than, say, 5/2 this becomes

$$\frac{(\sigma_o)_{max}}{p} = \frac{k}{2} \sqrt{6 \frac{E_c}{E} \cdot \frac{t}{\eta}} + k' \frac{t}{c} \cdot \sqrt[4]{6 \frac{E_c}{E} \cdot \frac{t}{\eta}} \quad . \qquad (10)$$

Figure 14 is a plot of $\frac{(\sigma_o)_{max}}{p} \frac{c^2}{t}$ versus λ for various values of k. The increasing overlap ratio $\frac{c}{t}$ results in decreasing values of the maximum tearing stress $(\sigma_o)_{max}$ at the end of the joint.

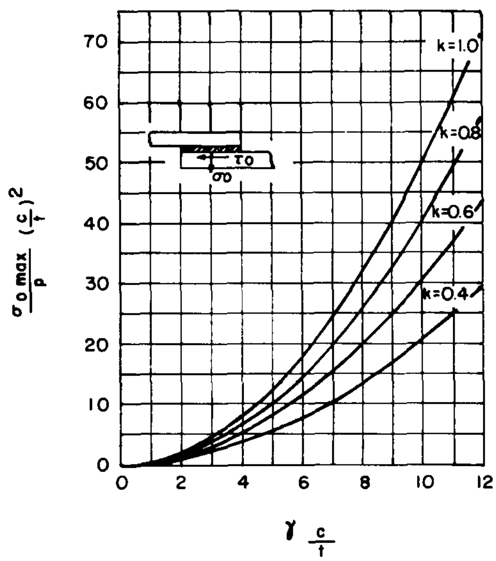

Figure 14. Maximum Tearing Stress in Adhesive in Joints with Relatively Flexible Adhesive Layers[19]

(4) Ranges of Validity of Approximations. The first approximate theory considered joints with thin inflexible adhesive layers, while the second approximate theory considered joints with flexible adhesive layers. Goland and Reissner studied ranges of validity of these approximations on the basis of a strain-energy concept.

The first approximate theory, which neglects the flexibility of the adhesive layer, was found to be acceptable when the following conditions are satisfied:

$$\frac{\eta}{E_c} << \frac{t}{E}, \qquad \frac{\eta}{G_c} << \frac{t}{G} \quad . \tag{11}$$

The second approximate theory neglects, in effect, the strain energy due to stresses in the adherend, σ_y and τ_{xy}, compared with the strain energy due to stresses in the adhesive, σ_o and τ_o. The second approximate theory was found to be acceptable when the following conditions are satisfied:

$$\frac{t}{E} << \frac{\eta}{E_c}, \qquad \frac{t}{G} << \frac{\eta}{G_c} \quad . \tag{12}$$

However, many metal joints with organic adhesives which are presently used for aircraft and other structures do not satisfy either one of the conditions given by Equations (11) and (12).

d. Modifications of the Goland-Reissner Theory

(1) Plantema's Modification. An attempt to combine the Goland-Reissner theory with that of Volkersen was made by Plantema.[4,20] He used the Volkersen analysis to determine stress distribution at the ends of the lap joint due to the differential straining of the members. From this, he calculated the bending moment and its resulting stress in the adherends at the edge of the lap joint. The Goland-Reissner theory was used to find the deformation of the adherends. Plantema derived the following formula for the stress concentration factor, n:

$$n = \omega \coth \omega \ , \tag{13}$$

where

$$\omega = \frac{1}{2}\sqrt{1 + 3k} \ . \ \frac{\beta c}{t} \quad . \tag{14}$$

Figure 15 shows the variation of n with ω, where ω changes between 0 and 4. When $\omega > 4$, $n \simeq \omega$.

(2) Cornell's Modification. Cornell[22] used the Goland-Reissner theory as a basis for work on stress distribution in cemented or brazed lap joints. He used a joint system as shown in Figure 16 and made the following assumptions in regard to it:

1) The two adherends act separately according to simple beam theory.
2) The adhesive layer is the same as an infinite number of shear and tension springs.

3) The deflection of the specimen is slight compared to its dimensions and has no influence on the loading of the joint.
4) The free adherend is long enough that it will not affect local stresses at the end.
5) The adhesive layer is so thin that its beam thickness can be ignored.
6) The two adherends are narrow (each a unit wide).

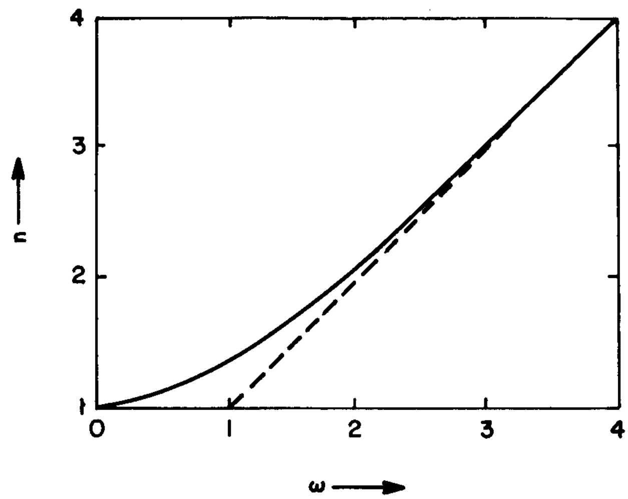

Figure 15. Variation of n with ω[4]

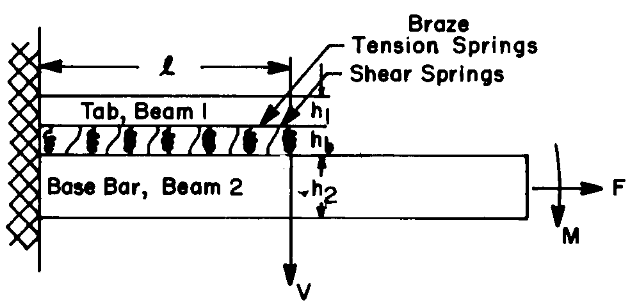

Figure 16. Schematic Drawing of the Joint Considered by Cornell[4]

In this system, there is a transfer of the load from one adherend through the spring system to the other adherend. Cornell described this transfer by a series of differential equations. These were then reduced to a pair of ordinary linear differential equations with easily found solutions.

Cornell's work also indicated a high stress concentration around the joint end. He compared his results to those of photoelastic and brittle lacquer experiments and found that his system gave a fairly accurate picture of stress distribution.

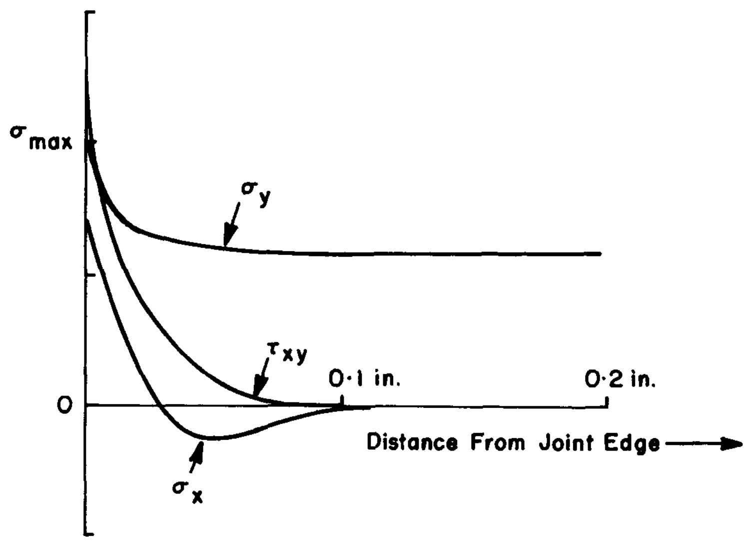

Figure 17. Stresses at the Adhesive Surface in the Lower Adherend in the Case of Pure Bending

2. Lap Joints Under Loads Other than Tensile

This paragraph discusses briefly the effects of loads other than tension on lap joints.

a. Lap Joints Under Bending

Due to the eccentric loading, as shown in Figure 3, bending moments are produced in a lap joint subject to tensile loading. Consequently, some of the analytical methods developed primarily for studying stress distributions in lap joints under tensile loading can be used for studying stress distributions in lap joints under bending.

Figure 17 illustrates results obtained by Cornell[22] for stresses in the adhesive surface of the lower adherend under pure bending. The model used by Cornell is shown in Figure 16. The case shown in Figure 17 corresponds to the following values:*

$h_1 = 0.04$ inch, $h_t = 0.01$ inch, $h_2 = 0.25$ inch

$E_1 = E_2$ (Young's modulus of adherends) $= 3 \times 10^7$ psi

$E_a = 1.5 \times 10^7$ psi, $G_a = 5 \times 10^6$ psi.

Sherrer[21] and Ito[27] also studied stress distributions in lap joints subjected to bending loads. Assuming that adherends act as cylindrically bent plates, Hahn and Fouser[28] determined stress distributions outside the bonded area. Their results show, as have others, that maximum stress distribution is at the edge of the overlap.

b. Lap Joints in Edgewise Shear

In aircraft structures, wide lap joints are often loaded asymmetrically parallel to the lap.[10] In this case, adherends bend in the plane of the sheet. Ljungstrom[29] suggested that stress distributions in lap joints in edgewise shear can be obtained by using the sheet shear modulus instead of Young's modulus in Volkersen's formula. This has been supported by test results.

c. Matrix Structural Analysis

A recent method of analyzing lap joints is that of matrix structural analysis.[13] Lobbett and Ross[30] were the first to apply this technique to the lap joint problem. Its basis is a network model of a lap joint made of bar and shear panel elements. Such a model can be made to idealize completely a lap joint, and it can be subjected to any loading situation. The behavior of each element is written in equation form and these equations solved simultaneously for the entire network. The solutions are then placed in computer language by use of matrix algebra. By use of the computer, a great number of calculations concerning stress distribution can be made, many of which could not be attempted with any other method.

Goodwin[31] has used this method to investigate the effect of joint parameters on elastic stress distribution in a lap joint, including length

*The values are for a brazed joint.

of overlap, braze (adhesive) modulus, film thickness, joint support, adherend taper, and air-braze interface radius. Goodwin's study was concerned with brazed joints, but the results could be applied to the more flexible adhesive joints.

3. Joints Other than Lap Joints

The following paragraph contains short summaries of work relating to stress distribution in other types of joints.

a. Butt Joints

The adhesive layer in butt joints is subject to lateral constraint unless both the adherends and the glue have the same ratio of Poisson's ratio to Young's modulus.[10] In metal-to-metal bonds, stress distribution will depend upon dimensions of the bond area and their relation to the adhesive thickness. This is because the adhesive, being of lower order of modulus than the adherends, will be subject to lateral constraint. DeBruyne[32] reported joint strength to be inversely proportional to thickness for very thin adhesives. He obtained experimental agreement for this relationship. Shield[33] used limit analysis to study strength in butt joints.

b. Scarf Joints

Stress concentrations in a simple scarf joint are very small, but as scarf angles increase, the lateral constraint described with butt joints occurs.[10] For most angles, there is also a problem of finite shear stress at the boundaries. Cooper, using strain measurements of the adherends, found that a shear stress concentration factor of 1.45 existed for six-degree scarf.[4] Hartman[34] and Muller[35] have done work on the interaction of shear and normal stress, which they found to be more important in scarf joints than in lap joints. Lubkin[36] has developed an analysis to confirm experimental results in regard to scarf joints and has also considered the problems of lands on scarf joints.

c. Tubular Joints

Lubkin and Reissner[37] produced an analysis for distribution of stress in adhesive lap joints between tubes.[10, 25] Their analysis allowed for radial contractions and expansions outside the joint, much like the bending Goland and Reissner considered for lap joints. The analysis applies primarily to bonding of metals and plastics, as the investigators treated the adhesive as a thin elastic layer, much more flexible than the tubes. The results show shear stress concentrations for thick tubes that are close to those of Volkersen.

Perry[9] has found that results of analysis of flat scarf joints may be applied with accuracy to tubular scarf joints in tension or bending.

Section IV. EXPERIMENTAL STRESS ANALYSES OF ADHESIVE-BONDED JOINTS

1. Background

It is very difficult to find the stress distribution in a bonded lap joint by experiment. This is particularly true for the adhesive, which is only about 0.010 inch thick.[13] Not only is the adhesive in a very thin layer, but most of it is hidden by the surfaces of the adherends - only a minute fraction is exposed at the edges of the joint. There is no currently available device for measuring stress that can be practically applied to such a small area, and drilling into the adherends to expose more adhesive alters the bonding properties and influences any test results.

Because of this, most studies have used large models of joints. The assumption is that results obtained on these models will be true for the actual joint. One question remains completely unanswered regarding this assumption. Does an adhesive behave the same mechanically in an 0.005-inch film as it does when enlarged to 0.500 inch? Whatever the answer to this question, any model of a joint should meet the following conditions:[13]

1) Maintain the ratio of adherend thickness to adhesive thickness of the actual joint.
2) Maintain the same ratio of adherend shear modulus to adhesive shear modulus, or the general ratio of mechanical properties of adherend to adhesive, as the actual joint.
3) Be wide enough to ensure a condition of plane strain in the plane of the adhesive.
4) Simulate a true adhesive bond between the adherend and adhesive. It is important to simulate the discontinuous nature of the mechanical properties at the adherend-adhesive interface.

a. Techniques Used

Three techniques have been generally used for experimental study of stress distribution in bonded joints. Two of these use joint models, as described above. The most common technique uses loads applied to models made of photoelastic materials, with stresses determined photoelastically. A second technique uses gelatin and rubber models, with stresses measured by grid systems. This is much less reliable and has received very limited use. The third technique allows studies to be made on actual adhesive-bonded joints. This is a recently developed method using photoelastic coatings.

b. Results of Experimental Studies

Experimental studies have proven that elastic stress concentrations exist at the ends of the joint overlap. In some instances, it has been possible to relate this to the mechanical properties of the adhesive.[13] Studies have also demonstrated the existence of a nonuniform stress distribution across the width of the joint. Figure 18 shows the complexity of stress distribution in the adhesive film of a lap joint. Shown are τ_{xy}, shear stress in the x-surface in the y-direction, and σ_y stress normal to the y-plane.

There are several important factors that have not yet been shown experimentally.[13] These include stress distribution in the joint beyond the elastic limit of the adhesive or adherends, the relationship between stress distribution throughout the joint, and the ratio of mechanical properties of the adhesive to those of the adherend.

2. Analyses with Photoelastic Models

Coker[38] is credited with the earliest photoelastic study of joints. Although he was not studying lap joints, the model he used actually simulated a double-lap joint, so his experiment is of interest. Coker's setup consisted of three parallel sets of steel bars bolted to a plastic sheet, as shown in Figure 19. The ratio of Young's modulus of the steel to that of the plastic was 10.

Measurements were made using transmission photoelasticity. These were taken along the centerline of the bond area to determine the effect of film thickness and length of overlap on shear strain. The results showed that shear strain increased sharply from zero at the end of the overlap to a maximum at a point very near the end, and then fell off to its minimum at the center of the overlap. Changing film thickness did not appear to change this pattern, but it did have an effect on stress distribution near the ends of the overlap.

Another early photoelastic study was that of Tylecote,[26] who found high shear and normal stresses near the ends of the overlap in plastic models of spot-welded joints. The maximum shear-stress concentration was 5.7. The joints in Tylecote's models, cut from a single plane sheet of plastic, compared to an adhesive-bonded joint in which the adhesive and adherend had the same physical properties. Since properties were the same within the joint, the offset in the geometry of the lap joint had a marked effect on stress concentration.

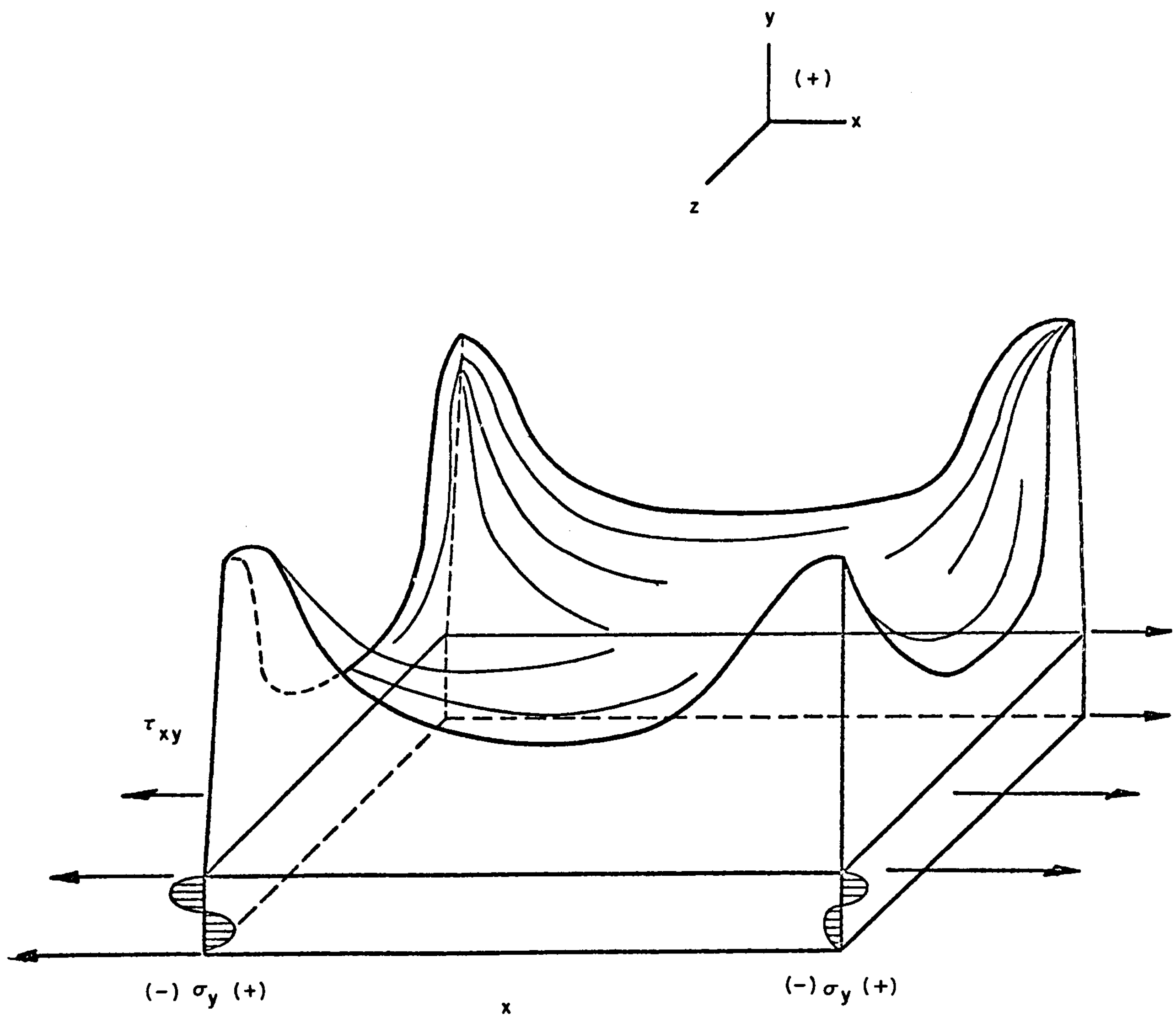

Figure 18. Three-Dimensional Plastic-Shear Stress Distribution in the Adhesive Film of a Lap Joint[13]

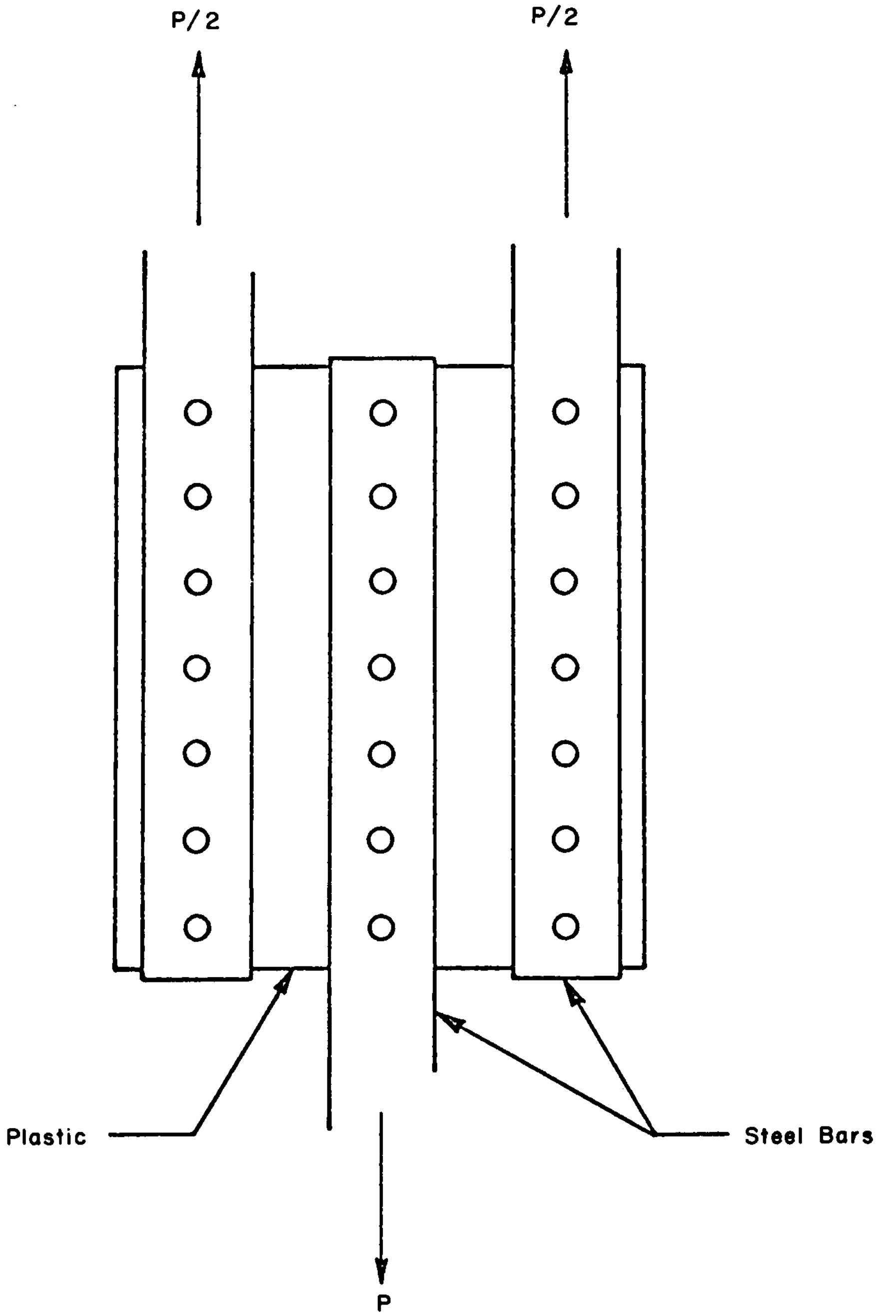

Figure 19. Photoelastic Model Simulating a Double Lap Joint used by Coker[13]

In 1948, Mylonas[39] published results of the first systematic attempts to study stresses in an adhesive by means of photoelasticity. Mylonas had first made models with wood adherends, using a layer of Catalin 800 plastic as the bond. Because of difficulties in making stress-free joints, little analysis was done. Most of his early experiments were performed on models made from single sheets of Catalin 800 machined to a desired shape. With these models, steel strips were bolted to the plastic, as in Coker's studies. These served to stiffen the plastic and better simulate a joint. Mylonas concluded from these studies that the most critical stresses were at the interface areas at the end of the overlap. The stress concentration factors, measured photoelastically, were generally lower than calculations made for the same models using Volkersen and Goland-Reissner analyses.

In the models mentioned above, Mylonas had made the air-adhesive (or end-of-overlap) interface curved. He later conducted further study on stress distribution along this interface.[40] For these studies, he made models with curved air-adhesive interfaces of different radii. He also made models with straight interfaces, but varied the degree of slope for these (Figure 20).

From these studies, it was concluded that for joints with a large radius, failure would occur along the adhesive-adherend interface. For a small radius, failure would most likely occur in the adhesive. For the straight interfaces, stress decreased as the angle of slope decreased, being highest when the angle was 90 degrees to the plane of the adherends.

In this same series of studies, Mylonas made models with varying lengths of overlap to see what effect this factor would have on stress distribution. The adherends in these models were practically rigid. Theoretically, this nearly infinite stiffness, combined with the finite length of overlap, should lead to a uniform shear throughout the adhesive layer. When overlap length was at least three times the width of the joint, stress distribution was not affected by varying this length. So long as this ratio was held, there was an area of uniform stress in the center of the adhesive layer. With this knowledge, Mylonas kept the length-to-width ratio well over three to one in subsequent experiments mentioned above.

Mylonas also did some work on stresses in butt joints. For these tests, he used a model made of an adhesive layer fixed to two rigid, parallel surfaces. The adhesive was subjected to a tension normal to its plane by these surfaces.

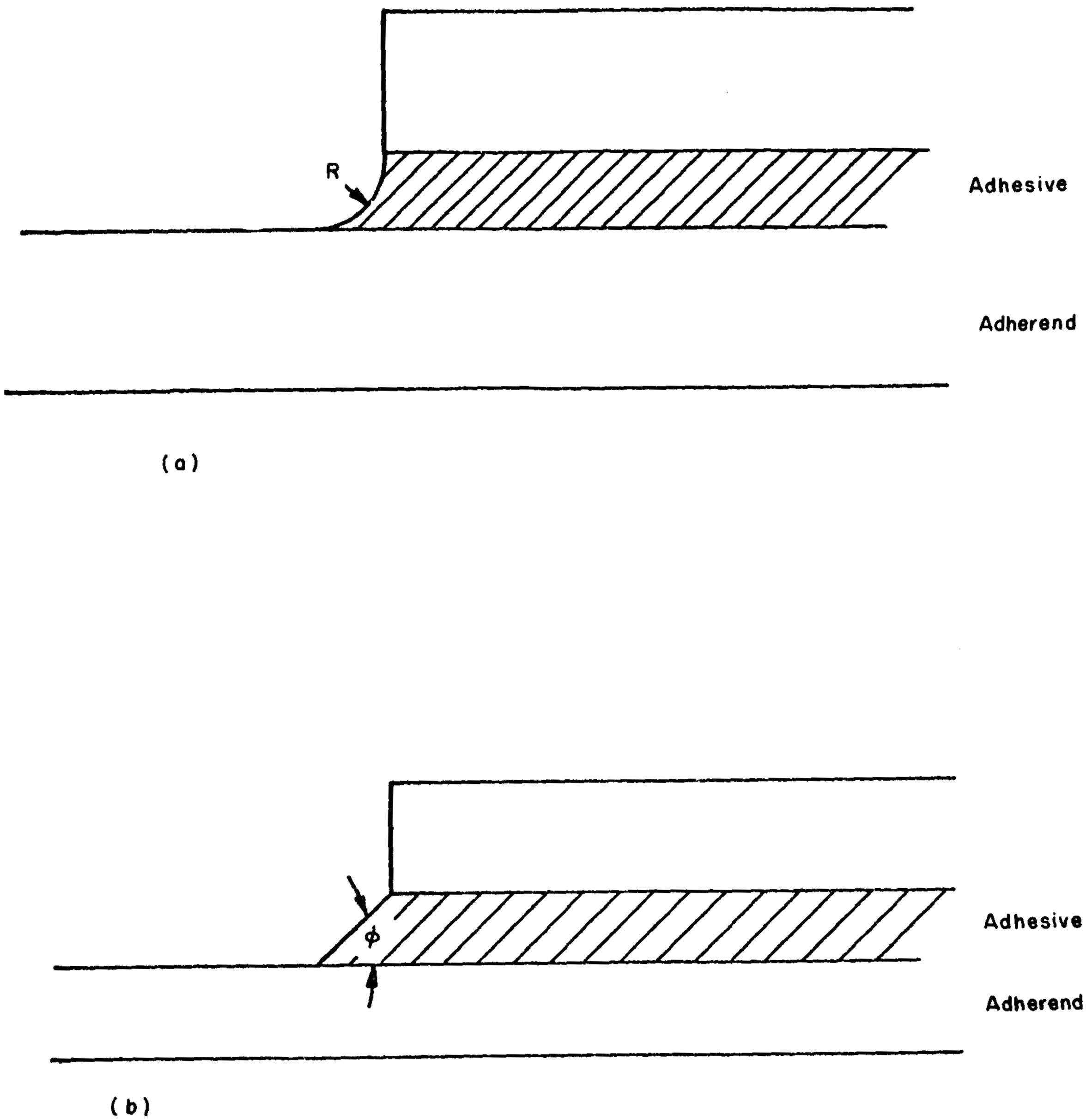

Figure 20. Two Typical Air-Adhesive Interfaces in Lap Joints: (a) Curved; (b) Linear[13]

McLaren and MacInnes[41] have made an extensive study of the effect of bending on stress distribution using photoelasticity. To accomplish this, they ran tests on two different model types. The first type consisted of single-sheet models cast in Araldite and simulating a lap joint with one-half-inch-thick adherends and an adhesive layer varying from zero to one-half inch thick. The second type was made of two different plastics, with the adherends 20 times stiffer than the adhesive. In these experiments, as in the Goland-Reissner theory, it was assumed that the only effect of the load on the geometry of a joint is to produce a rotation of the joint about its center. If the line of action of the load T passes through the point E on AB in Figure 21, the effect of the rotation can be determined by the factor K = BE/CB. The effect of varying K can be investigated by changing the direction of the applied loads.

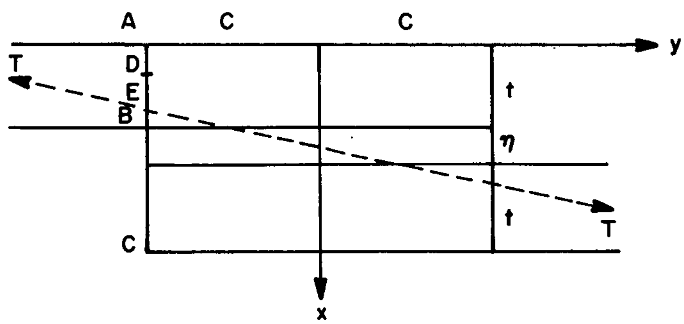

Figure 21. Diagram of Joint to Which Load Is Applied as a Distributed Boundary Stress by Adherend

In both model types, when K was a positive factor, the maximum stress concentration was at the ends of the length of overlap. This decreased to a minimum stress at the center of the joint. When the value of K was increased, the stress concentration at the ends increased proportionately, but remained about the same at the center. For negative values of K, the opposite was true, again for both model types. Stress concentration could almost be eliminated at the ends of the overlap but increased toward the center of the overlap. After considering these results, McLaren and MacInnes felt that a lap joint with negative K might have merits. Experiments on such a joint (Figure 22) showed that stresses are greatest at the center of adhesive-adherend interfaces and that they decrease toward the free surfaces.

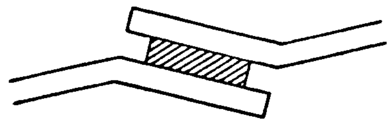

Figure 22. Lap Joint with Negative Bending Moment Factor[24]

A difference between the two models was found in the results when K = 1, or when the line of the applied load passes through the centerline of the adherend at the end of the bonded area. In the homogeneous model, principal stresses were parallel and perpendicular to the line of the joint except at the very ends of the overlap. This was true in both the adhesive and adherends. This means there was no shear transfer of load across the bond line along the central area of the joint. In the composite model, the directions of stress were the same in the adherends, but were at 45-degree angles in the adhesive. This shows that, except at the ends, the adhesive was mainly in longitudinal shear. This would indicate that homogeneous models simulate conditions in actual joints accurately. An exception would be a joint in which adhesive and adherend had matching properties - not a practical application.

In the course of this study, McLaren and MacInnes found support for Mylonas' conclusions on the effect of slope of the air-adhesive face. There was also a suggestion that higher values of K might result in less tensile strain in the adhesive surface.

The main value of the work of McLaren and MacInnes is the suggestion that by changing the bending moment factor, one can reverse the stress concentration in the edges of a bonded joint. This could be of considerable interest in joint design, as shown in their experimental lap joint.

Kutscha[42] also made some photoelastic investigations of shear stresses in composite models of lap joints. He attempted to approximate more closely an actual joint, especially in film thickness. By use of photoelastic analysis, he was able to study stress distribution on the adhesive itself. Using liquid Photostress A, he made lap joints of 0.064-inch-thick aluminum alloy with an adhesive film thickness of 0.029 inch. The joint width was 0.25 inch. Measurements of the effect of length of overlap on shear stress distribution were made. These results were compared with the distribution predicted by the Goland-Reissner analysis and were found to be generally higher. In the analysis, shear modulus for the adhesive was determined on bulk material rather than on a film in a joint. This leaves some question concerning the comparison.

In a continuation of this work, Kutscha[43] found that maximum shear stress in the joint is directly related to adherend thickness and length of overlap, or joint parameter L/t. The relationship was true for a series of joints with the same adherend thickness, but not for a group with different thicknesses. This indicates that the joint parameter L/t is not a proper reflection of the bending moment in the joint. Kutscha also analyzed joints with the adherends tapered along the length of the overlap. This might be expected to correct differential straining and reduce stress concentration. However, the analysis did not show this to be true. It was suggested that this be studied further, with the taper thickness adjusted to correct the differential straining condition exactly.

3. Analyses Using Gelatin and Rubber Models

Stress distribution has also been measured using gelatin or rubber models. This is not a reliable technique, but has been used by several researchers whose work is reviewed here. The earliest work that can be related to lap-joint analysis was performed by Andrade[44] using gelatin. This study was not set up to analyze lap joints, but the conditions of the experiment made the subject similar to a simple lap joint without loading. Andrade used a gelatin block to test shear stress. The block was 4 by 4 by 16 inches. Two wooden boards were bonded to it along its long sides. A shear load was applied through these boards. Grid reference marks were placed on the gelatin surface and shear strains noted by measuring changes in these marks. Results showed shear strain to be greatest near the edges of the overlap and least towards the center of the joint. Shear strain across the adhesive varied from one adherend to the other. The maximum shear-strain concentration was about 1.25.

Jackson[45] used lap joint models cut from pieces of low-modulus rubber in another approach. The joints were homogeneous. Jackson sought to show the effects of changes in joint geometry on strains in lap joints. The strains he illustrated were actually those in the adherends.

Norris and Ringelstetter[46] made a model to simulate the bond between the skin and cap strip in a wooden aircraft wing. Measurements of shear strain were made along the glueline of this double-lap joint using a Tuckerman optical strain gage. Maximum shear strain was found at the ends of the overlap.

The effect of applied load on stress distribution in a lap joint was measured by Demarkles[47] using foam rubber. Two pieces of foam rubber were bonded with an adhesive having the same mechanical properties. A grid was painted on the surface of the rubber. When a load was applied, strain measurements were made by noting the changes in the grid. By this method, shear stress in the adherend (not the adhesive) was measured. The results were compared with a Volkersen analysis and found to be lower than predicted.

4. Analyses with Photoelastic Coatings

By use of photoelastic coverings, stress measurements may be made on actual joints. Hahn[24] used this technique on aluminum lap joints bonded with Metlbond 4021. He was seeking to find the stress distribution in the adherends just adjacent to the bond area, and by use of of a reflective photoelastic coating was able to do this experimentally. Hahn used joints made of aluminum pieces one-fourth by two by eight inches in size, with a joint overlap of two inches. The experimental results compared very well with a mathematical analysis.

The results of this work were important in two areas. First, it was found that the adherends showed an inelastic deformation just outside the bond area. This is believed to be due to the concentration of shear stresses at the edges of the adherend. Shear stress distribution, then, is not uniform across the width of the adherends.

A second important result was the indication that this inelastic curvature is also present within the bonded area. If this is true, it means that shear stress varies across the width of the adhesive as well as along the length of the overlap. This appears to be true, expecially at the ends of the overlap. If so, a joint two inches wide is not twice as strong as a one-inch-wide joint. This could be very significant, and further investigation is needed in this area.

Section V. RHEOLOGY OF ADHESIVE-BONDED JOINTS

1. Background

Rheology is the study of the deformation and flow of matter. Actually, deformation and flow are closely related. Deformation is defined as a movement of particles in relation to one another without destroying the continuity of the body of material. The material flows if this deformation increases continuously with time. There are three branches of rheology. Phenomenological rheology considers homogeneous and isotropic materials as continuous media. Macrorheology regards all materials as being homogeneous as they might look to the naked eye. Microrheology studies behavior of multiphase systems from known rheological action of their parts. Reiner[48] wrote a review on fundamental problems of rheology covering the above three branches.

In regard to adhesives, two different problems exist. The first problem concerns the rheological behavior of adhesives during bonding. Deformation and flow are important in forming a bond using a liquid adhesive. The second problem concerns rheological behavior of adhesives when loads are applied to adhesive-bonded joints after they are bonded. A number of articles have been written on both aspects of the rheological behavior of adhesives.[4,6,24] This report is concerned with the second problem only, that is, the rheological behavior of adhesive-bonded joints subjected to external loading, and covers briefly the following subjects:

1) Simple viscous phenomena in separating two surfaces.
2) Complex viscous phenomena in separating two surfaces.
3) Visco-elastic phenomena and the separation of surface (tack).

Details discussed are given in Adhesion edited by Eley.[25]

2. Simple Viscous Phenomena in Separating Two Surfaces

The force required to separate two rigid surfaces joined by a viscous liquid is sometimes referred to as an adhesive force. The application of force to an adhesive-bonded joint could result in separation in one of the following three ways:[24]

1) A clean separation of one of the surfaces from the liquid.

2) A removal of one surface, dependent on time, together with viscous flow of the liquid between the surfaces.
3) A removal where some of the liquid remains on both surfaces due to cohesive failure.

Only the first way involves true adhesion, but it does not involve rheological explanation as do the other two. Therefore, only the latter two will be considered here.

Several authors, including Stefan[49] (as early as 1874) and, more recently, Bikerman,[50] have shown that the rate of separation in case (2) is a function of the viscosity of the adhesive and the force applied. The force needed to separate in this case varies directly with the rate of separation. This is shown in Equation (15),

$$\frac{dD}{dt} = \frac{2FD^3}{3\eta r^2} , \tag{15}$$

where D is the distance between two disc surfaces of radius r, and F is the force required to separate them. Banks and Mill[51] have shown that above a critical rate of separation, negative pressures exist which result in a maximum limiting force. This resistance to separation is called tack and will be discussed later.

3. Complex Viscous Phenomena in Separating Two Surfaces

For most adhesive, the ratio between rate of shear and shearing stress varies with the rate of shear.[24] Additionally, many of these adhesives cannot be sheared by stresses below a certain limiting value known as the yield point. The equation

$$\eta \cdot \frac{d\sigma}{dt} = (F-f)^n \tag{16}$$

summarizes this behavior, where $d\sigma/dt$ is the shear rate, F is the shear stress, f is the yield point, and n is a constant characteristic of the material. The parameter η is usually referred to as plasticity rather than viscosity, and is only constant for a Newtonian liquid, for which $f = 0$ and $n = 1$.

Scott[52] derived a formula for dD/dt as follows:

$$\frac{dD}{dt} = \frac{AF^n D \cdot D_o^{n+1}}{\pi^n r^{3n+1} \eta^n} \tag{17}$$

where

D_o = the limiting thickness achieved when a material with a yield point f is compressed between two parallel plates:

$$D_o = \frac{2\pi r^3 f}{F} .$$

A = an infinite convergent series and is a function of η and D/D_o. Then the force, F, required to separate the joined plates is

$$F \propto \left(\frac{dD}{dt}\right)^{\frac{1}{n}} \frac{\pi\eta^{3+\frac{1}{n}}}{D^{\frac{1}{n}} D_o^{1+\frac{1}{n}}} . \quad (18)$$

Peek[53] analyzed a simpler case for n = 1. He derived the following formula for the force F:

$$F = \frac{dD}{dt} \cdot \frac{4\pi\eta r^4}{3D(D-D_o)^2} . \quad (19)$$

These cases indicate that introducing a yield point has more influence on separating parallel surfaces joined by an adhesive than does departure of the exponent from the Newtonian value of unity.

4. Visco-Elastic Phenomena and the Separation of Surfaces (Tack)

Equation (16) describes only viscous behavior of adhesives when subjected to simple shear. These adhesives also show elastic behavior.[25] They will respond to the applied stress with a mixture of elastic deformation and viscous flow. It is the purpose here to discuss this visco-elastic behavior as it relates to tack. Tack is defined as the resistance to separation. However, it is not clear what properties in a material account for its presence. Many feel that tack depends on a different set of properties for different substances. Therefore, it can be judged only by bringing the adhesive into contact with a material. If clean removal of the material is impossible, or requires effort limited only by failure at the interface, then tack is present in the adhesive.[25]

By looking at how tack is exhibited in several different materials, we can see how it differs and why it has defied an agreed analysis. In

Printers' Ink, Green[54] has defined tack as pull resistance, while Banks and Mill[51] felt it is explained entirely by viscous flow. Carpenters' glue, with long chainlike molecules, has the ability to pull into long filaments, which results in tack. Unvulcanized masticated rubber has the property of self-diffusion of polymer chains. When two surfaces of the material are brought lightly together, their fusion obliterates their separate surfaces. Finally, there are pressure-sensitive tapes which strip cleanly from solid surfaces to which they should stick tightly.

It is known that tack is dependent on temperature and that many substances become "nontacky" below certain temperatures. In this regard, McLaren, et al.,[55] worked with three amorphous high polymers and found that at the tack temperature their melt viscosity was the same. At an applied pressure of 20 psi, polystyrene at 106°C, polyvinyl at 49° to 66°C, and polyisobutene at -32° to -36°C all had a viscosity of about 10^8 poises. It should be noted, however, that several extrapolations were involved, and the viscosity measurements were taken at much higher temperatures and pressures.

The drawing out of filaments, as in Carpenters' glue, is mentioned above. This phenomenon seems to be elastic in nature, as the filaments retract when adhesion fails. For an element of tacky substance whose length extends from ℓ_o to ℓ_1 before adhesion fails, the work of adhesion will be equal to the elastic energy stored in the tacky element at the moment of failure.[25] The deformation due to viscous flow will be given by

$$\log\left(\frac{\ell}{\ell_o}\right) = \frac{S_o\tau}{3\pi\eta r^2}\left(1 - e^{-\frac{t}{\tau}}\right) \qquad (20)$$

where

r = radius of the cylinder
s_o = stress applied at the end
τ = Maxwell relaxation time
t = time elapsed since the beginning of the extension.

The elastic energy stored, W, will be a function of the extension ratio $\frac{\ell - \ell_o}{\ell_o} = \lambda$ given by[56]

$$W = C_1\left(\lambda^2 + \frac{2}{\lambda} - 3\right) + C_2\left(\frac{1}{\lambda^2} + 2\lambda - 3\right). \qquad (21)$$

Where there is rapid extension of small elements, t/τ will have a fractional value, since the relaxation time for polymeric materials will be at least 0.01 second, and usually much longer. Thus, some of the deformation must be elastic and the energy stored proportional to the square of the extension ratio. The elastic component can be ignored only if extension is about twice the relaxation time, or more.[25]

Dow[57] has shown that stripping force for pressure-sensitive tape is proportional to the square root of the speed at which it is stripped.

Section VI. FRACTURE OF ADHESIVE-BONDED JOINTS

1. Background

Before discussing fracture of adhesive-bonded joints, a brief discussion is given on fracture of solids. The various theories of fracture of metals and other solids are classified as follows:

1) Continuum mechanics theory.

    a) Classical theories of fracture.
    b) Fracture mechanics theories.

2) Microstructural theories.
3) Atomistic mechanics theories.

In any study of fracture criteria, distinction is made between initiation of fracture and propagation of fracture.

The aim of continuum approach is to describe material properties in terms of limiting stresses and strains, to meet the needs of the designer. A material is considered as a continuous homogeneous medium, and the fracture is treated on a macroscopic scale. The classic theories under this approach explain that fracture occurs when the stress, the strain, or a parameter determined by the stress state reach a certain value for the particular material. Several criteria have been offered to explain various types of fractures in different materials. A book written by Nadai[58] contains much of the earlier, primarily European, work of flow and fracture of solids.

The fracture mechanics theories are based on Griffith's[59] work and have been developed by Irwin[60, 61] and other investigators. In these theories, studies are made on the balance between strain energy supplied from the stress system and the energy required for the initiation of fracture.

In the microstructural approach, studies are made of microscopic details of how the fracture process is nucleated and how microscopic fracture nuclei increase in size and produce complete failure. Microscopy, especially electron microscopy, is used extensively to study mechanisms of fracture. A recent review by Low[62] provides a good coverage of this area.

Using the atomistic approach, studies are made of how atoms in a solid behave under stress. It is known that a material's actual strength is two to three orders of magnitude lower than its theoretical strength based on the atomic binding force, which is about one-tenth of Young's modulus. The emphasis of studies is placed on the role of atomic imperfections, such as dislocations, on the deformation and fracture. Griffith's basic concept has been used in both the macroscopic and atomistic theories.

There are reports of several symposiums and conferences that offer excellent material on the recent development of theories of fracture. The proceedings of the 1959 Swampscott Conference[63] constitute the first successful stock taking of present knowledge, with emphasis on atomic and microscopic mechanisms of fracture. Conferences held at Maple Valley[64] in 1962 and Sendai[65] in 1965 included reviews on progress made with the different approaches mentioned above. The bulk of the information in the above sources refers to metals and ionic crystals, but fractures in glasses and polymers also were discussed. The monographs edited by Rosen[66] and Weiss[67] are directed toward fundamental problems of fractures in polymeric solids.

Only limited studies have been made on mechanisms of fracture of adhesive-bonded joints. There have been several attempts to apply classical fracture theories. Beyond these, however, very few articles exist on fracture of adhesive-bonded joints. There have been only a few isolated attempts to apply either fracture mechanics or electron microscopic studies to adhesive-bonded joints, and no attempts at studies on an atomic scale.

The thermodynamic approach, which has been developed primarily to study chemical problems such as bonding energy, interfacial surface energy, and solubility parameters, also can be used for studying fracture of adhesive-bonded joints. Gardon[14] has extended the theory of Hildebrand to relate the solubility parameter and surface tension parameters to the work of adhesion and general level of bond strength. He reports on the many contributions to this field as they apply directly to the understanding of strengths of bonded joints. The status of this research is the general correlation of these parameters, neglecting the effects of structural features in the systems.

2. Classical Theories of Fracture Applied to Adhesive-Bonded Joints

As stated above, there has been very little done to determine fracture criteria and mechanisms for adhesive joints. This is in spite of the great amount of joint-strength data accumulated over the years.

One significant study was that of Lubkin,[68] who tried to explain the strengths of adhesive scarf joints. He studied theories of failure to determine which best explained the joint strengths and found that the maximum principal-stress explained experimental data best. This theory assumes that the joint will fail when the tensile strength of the adhesive is exceeded.

3. Fracture Mechanics Theories Applied to Adhesive-Bonded Joints

The application of fracture mechanics theories to adhesive-bonded joints is quite new. So far, only a few articles have been published. Ripling, et al.,[69, 70] studied fracture of joints of the aluminum-epoxy-aluminum type. Additional studies were done by Fowlkes and Wolock.[71] Irwin[61] discussed problems related to the application of fracture mechanics to the study of fracture in adhesive-bonded joints. A short description of fundamental concepts of the fracture mechanics theory is given in the next paragraph for the benefit of readers who are not familiar with the theory. Fracture mechanics theory was developed for homogeneous brittle solids. Recently, attempts have been made to extend its use to ductile materials by introducing additional corrections for the influence of plastic flow before fracture. Further, extension of this theory to the markedly different situation that exists in adhesive-bonded joints should be done only with the full knowledge of the limitations of this approach. However, recent attempts for the application of the fracture mechanics theory on fracture of adhesive-bonded joints are described in the following sections. It is emphasized that results are exploratory and far from concrete.

a. Fundamental Concepts of the Griffith-Irwin Fracture Mechanics Theory

The Griffith-Irwin fracture mechanics theory has been applied to some extent to the study of unstable fractures, especially of those in high-strength materials for aerospace applications. Figure 23 illustrates typical behavior of a metal sheet containing a transverse central crack subjected to uniform tensile loading.[72] For a small crack, fracture strength exceeds yield strength. Gross yielding is observed in the load-deflection diagram and extensive plastic deformation is observed in the fracture surface. However, fracture from a long crack occurs abruptly with negligible plastic deformation. The observed fracture stress decreases with increasing crack length. Unstable fracture occurs when the stress-intensity factor, K, reaches a value, K_c, which is characteristic for the material:

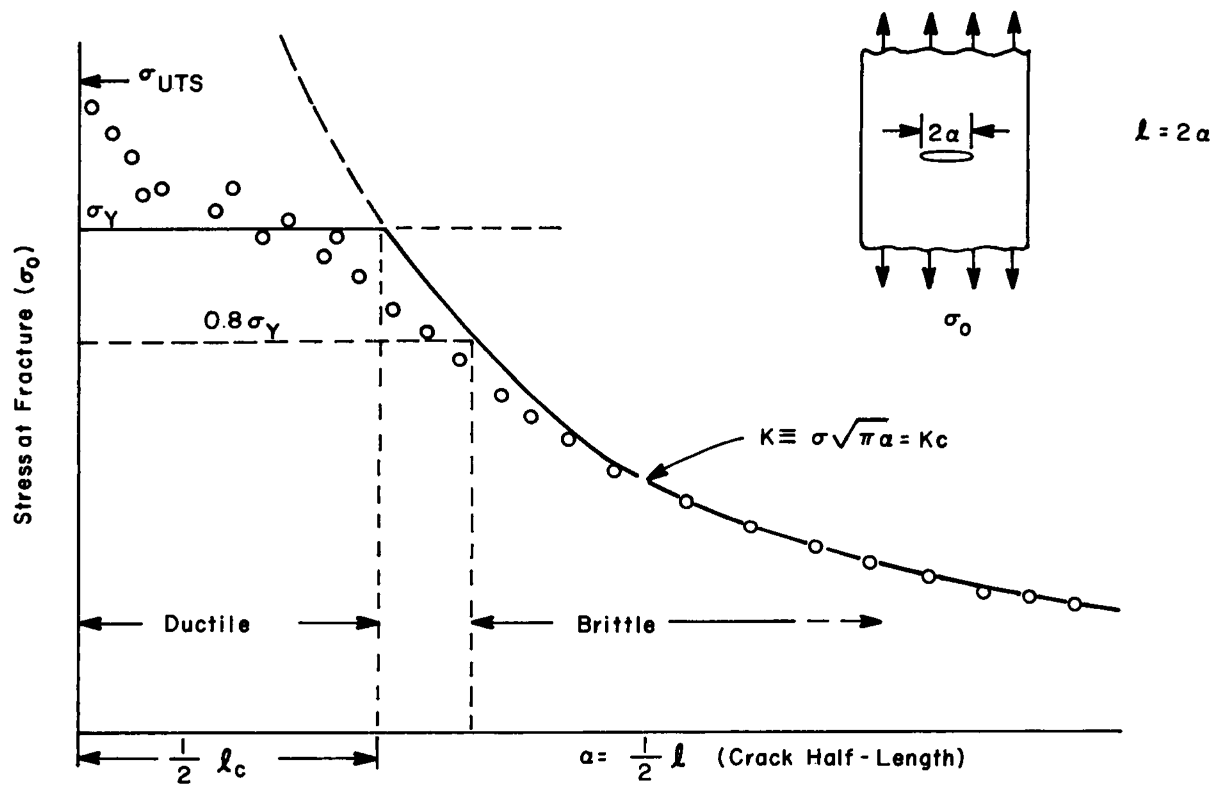

Figure 23. Effect of Crack Length on Stress at Fracture

$$K \equiv \sigma\sqrt{\pi a} = K_C \quad , \qquad (22)$$

where σ is average fracture stress and a is half crack length. K_c is called the critical stress intensity factor or fracture toughness of the material. The critical crack length, ℓ_c, also may be used to characterize the brittle behavior of the material when the preexisting crack is shorter than ℓ_c, fracture stress, σ, exceeds the yield stress, and fracture is ductile. The ASTM Committee on Fracture Testing of High-Strength Sheet Materials[73] has described methods of measuring fracture toughness of high-strength sheet metals (ferrous and nonferrous materials having a strength-to-density ratio of more than 700, 000 psi per pound per cubic inch). K_c can be determined by fracture tests of notched specimens. It has been found that as the tensile strength of a material increases, the critical crack length decreases, and the size of flaws tolerable in a structure decreases.

(1) Crack Tip Stress Fields for Isotropic Homogeneous Bodies. The stress fields near crack tips can be divided into three basic types,[74] each associated with a local mode of deformation, as shown in Figure 24:

Mode I: opening mode.
Mode II: edge sliding mode.
Mode III: tearing mode.

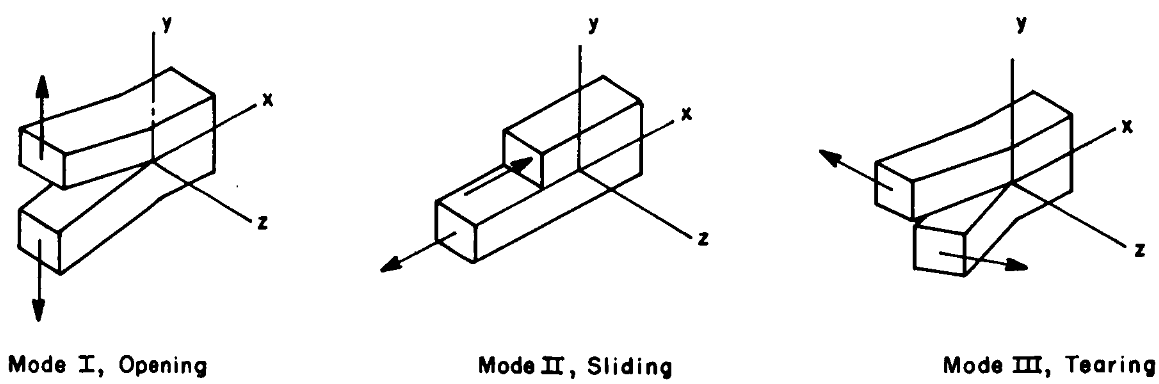

Figure 24. Basic Modes of Crack Surface Displacements[74]

The opening mode is associated with local displacement in which the crack surfaces move directly apart (symmetric with respect to the x-y and x-z planes). Displacements in the edge sliding mode find the crack surfaces sliding over one another perpendicular to the leading edge of the crack (symmetric with respect to the x-z plane). In the tearing mode, crack surfaces slide parallel to the leading edge (skew symmetric with respect to both the x-y and x-z planes). Even the most general case of crack tip deformation can be described by the superposition of these three modes. Irwin[75] has analyzed elastic stresses in areas near crack tips for the three modes. Paris and Sih[74] also have calculated stress fields for the three modes.

(2) Strain-Energy-Release Rate of Crack Extension. The elastic strain-energy-release rate of crack extension, g (in units of inches per pound per square inch) is often used instead of the stress-intensity factor, K. The relationship between K and g is:

$$g = \frac{(1-\nu^2)}{E} K^2 \quad \text{for plane strain}$$

$$g = \frac{K^2}{E} \quad \text{for plane stress} \tag{23}$$

where E is Young's modulus and ν is Poisson's ratio.

When there is enough stress intensity for K to equal K_c, the strain-energy-release rate becomes critical and g equals g_c. g_c then is defined as the amount of energy required to extend a crack of unit width one unit of length. A method for measuring fracture toughness was suggested by Irwin and Kies,[76] using this definition. They based it on an experimental calibration of a test specimen. The procedure measured total loss of strain energy through the propagating crack. In this case, the equation for g is

$$g = \frac{P^2}{2b} \frac{d\left(\frac{1}{M}\right)}{da} \tag{24}$$

where

b = specimen width

$\frac{1}{M}$ = compliance of the system

a = crack length

P = applied load.

If P is the critical load to move the crack a distance, P_c, g attains its critical value, g_c.

b. Fracture Mechanics of Adhesive-Bonded Joints

In a large block of isotropic material with a spreading crack, the separation will seldom be of a Mode II type.[61] In an adhesive-bonded joint, however, failure will remain within the joint under various stress conditions, since the adhesive is weaker than the adherends in most cases. In such a joint, critical g_{II} values can be easily measured and mixed-mode crack stress fields are usually found.

Figure 25 shows two blocks of separate materials, one of higher modulus, joined by a thin adhesive layer. If the two blocks are pulled in tension parallel to the joint, x-direction crack displacements next to the two walls will usually be different. Thus, crack surface displacements are not due only to the opening mode. They may be caused by a different ratio of modulus to Poisson's ratio for the two materials, or by residual stress, or by both. In any case, these additional displacements tend to help separation by increasing the strain energy release.

There are means for calculating values for K_I and K_{II} corresponding to the stress field for this figure. However, for most test situations, experimental analysis can furnish the same information easier and cheaper.

Irwin,[61] in seeking a means of testing adhesive joints, considered a joint as shown in Figure 25(b). It was assumed that the adhesive material, B, occupies such a thin layer that y-direction displacements in the material, A, at distances from the crack comparable to the crack length, correspond approximately to those which would be found for a crack of similar size and location in a solid specimen of A with the adhesive layer absent. The presence of the adhesive-bonded joint does not affect this analysis, as strains in the adhesive close to the crack edge can be explained as crack length correction.

Ripling, et al.,[69,70] used the specimen shown in Figure 26 for the same purpose. The specimens were aluminum-epoxy-aluminum joints. Because epoxy changes its response with time, they found it necessary to use a procedure allowing for a series of controlled crack extension speeds. The system they used allowed them to perform a peel test on the adhesive and to easily calculate g values. At the same time, it avoided large strains in one adherend or compressive strains which often occur in peel tests.

They accomplished this by exerting force through strong fingers separated by a stiff mechanical arrangement having the effect of a wedge.

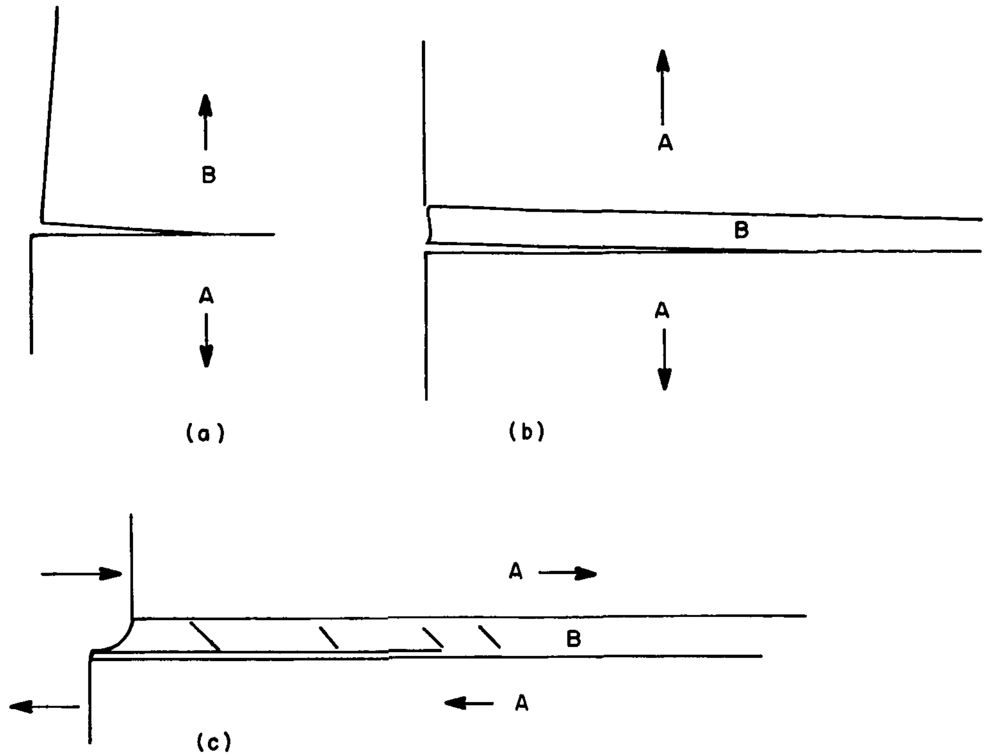

Figure 25. Separations from the Left Boundary in Adhesive Joints: (a) Thick Block of Material B Joined to a More Rigid Material A; (b) and (c) Thin Layer of Material B Between Block of Material A[61]

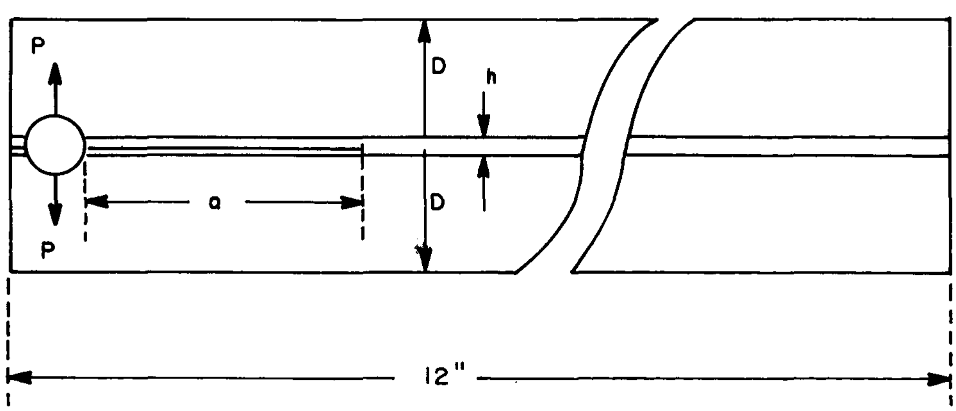

Figure 26. Ripling-Patrick Specimen for g_I and g_I plus g_{II} Measurements on Adhesive Joints. Most of the Specimen Bars Were 12 Inches Long and 1/4 Inch Thick, but These (as well as Other Dimensions) Are Arbitrary Choices[61]

They then measured the displacement separation of the force relative to zero load for various crack lengths. Compliance C (per unit specimen thickness) was then calculated by the equation

$$Y = \frac{CP}{B} \ , \qquad (25)$$

where Y is displacement separation, P the forces, and B the specimen thickness. Simple beam theory then shows

$$C = A(a + a_o)^3 \ , \qquad (26)$$

where

$A = 8/EBD^3$

D = depth of beam

a_o = radius of loading hole

E = Young's modulus of adherent material.

In such a joint, the "elastic foundation" will contribute to deflection from the adhesive. Allowing for this, compliance values agree basically with Equation (26). For comparison of compliance, saw cuts were made in solid aluminum bars to represent various crack sizes. Results of experimental stress analysis were shown by

$$C = A' \, (a + a'_o)^m \ , \qquad (27)$$

where the A', a'_o, and m values were adjusted for the data but differed only slightly from corresponding terms of Equation (26). Compliance data for this experiment can be represented by

$$C = A(a + a''_o)^3 \ , \qquad (28)$$

where a''_o is moderately greater than a_o and represents the effect upon compliance of the strains in the low-modulus component, material B.

Crack extension force is shown by

$$g_I = \frac{1}{2} \frac{P^2}{B} \frac{d}{da} (C) \ . \qquad (29)$$

g_I for any pair of P, Y observations can be computed, on the basis that the effective crack length is a value consistent with Equation (28) and with the observed values of P and Y. This is shown by

$$K = \frac{3}{2}\frac{PY}{B}\left(\frac{A}{BY}\right)^{1/3} BP \quad . \tag{30}$$

With Y fixed, the fractional change of crack extension force with a is given by

$$\frac{1}{g}\frac{\partial g}{\partial a} = -\frac{4}{a + a''_o}. \tag{31}$$

Much care is needed in preparing joints for measurements of the type being discussed here. Joints, as usually prepared, have non-uniform thickness, residual stress, voids, and surface condition. Also, high polymer adhesives are normally strain rate sensitive and tend to respond with greater stiffness and less toughness to rapid straining, as might occur with a rapid increase of crack extension. The joints discussed here must be partially precracked without completely separating them. So, a "stability factor" is needed even if they are carefully prepared. This term will be used for the left side of Equation (31). Ripling, et al.,[69,70] found in their aluminum-epoxy-aluminum joints that when a negative magnitude of the stability factor was much less than 0.5 reciprocal inch, unstable rapid fractures occurred. Stable crack extension was observed to a length of nearly eight inches, in consistency with Equation (31). If weaker, less uniform joints are to be studied, beams with less depth could be used.

g_I values for a series of joint thicknesses with a slow crack speed of about one inch per minute are shown in Figure 27. Where the adhesive is in greatest tension, there will be a tendency to contract in the specimen thickness direction. This tendency was strong enough to the right of g_I minimum in Figure 27 to cause a notching action which kept the crack plane near the middle of the joint height. The tendency to the left of this minimum was for the crack plane to stay close to an adherend surface. Here, the separation surface had a rougher appearance. It was not determined why g_I values drop for very small joint heights. However, the reasons are likely related to the nonuniformities noted above.

P and Y were also measured with the forces at a 45-degree angle relative to the joint. Values of g_I and g_{II} were estimated by using the components of P and Y normal and parallel to the joint. The total g value was much greater with shearing strains parallel to the joint. Also, the value of g_I was several times greater than under opening mode conditions.

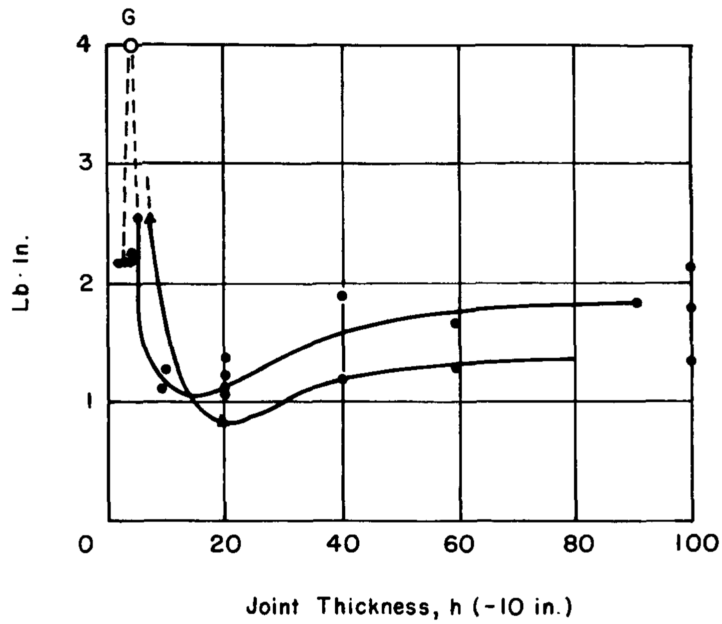

Figure 27. Effect of Joint Thickness h upon Critical g_I Values for Progressive Separation. Circle Points Were Measured with the Crack Speed Roughly One Inch Per Minute. Triangle Points Were Measured with the Speed Increased by a Factor of 25. Points on Right Margin Were Measured with Solid Epoxy Specimens[61]

It is not always possible to avoid compression and shear on adhesive joints in actual uses, although it is desirable. Hence, the critical value of g_I is of practical interest. However, more attention is usually given to the strength relative to shear separation. Ripling measured several values of g_{II} using specimens similar to that in Figure 26. Forces were applied as shown in Figure 25(c). Compliance for this experiment is a linearly increasing function of crack length, derived from

$$g_{II} = \left(\frac{P}{B}\right)^2 \frac{1}{ED} \ . \qquad (32)$$

The resulting g_{II} values were an order of magnitude greater than the g_I values in Figure 27. The instability restraint factor was only half that of the Mode I tests. Still, a long stable movement of the crack was observed.

The experiments show the need for a large negative stability factor in an adhesive joint test sample. This appears to be due to nonuniformities in the joint rather than merely low crack toughness. In glass, by way of contrast, a crack is easily extended in a controlled stable fashion by use of splitting forces near the plane of the crack. Crack speed can be controlled with only a small negative magnitude of the stability factor, although the necessary crack-extension force is less than 0.1 pound per inch.

4. Microstructural Studies on Fracture of Adhesive-Bonded Joints

During the last decade, there has been increasing interest in microstructural studies on fracture of metals and other solids. Electron-microscopic fractography, which is the observation under an electron microscope of fracture surfaces (in most cases, plastic replicas of fracture surfaces), has been proved to be very useful for studying micromechanisms of fractures.[62, 77] Limited attempts have been made by investigators, including Ilkka and Scott,[78] Reegen and Ilkka,[79] and Newman and Wolock,[80] to use the electron microscope to study microstructural characteristics of fractures in adhesive-bonded joints and polymers.[14] Such investigations should be extended to better understand micromechanisms of fractures of adhesive-bonded joints.

Section VII. EFFECTS OF LOADING AND ENVIRONMENTAL CONDITIONS ON DEFORMATION AND FRACTURE OF ADHESIVE-BONDED JOINTS

This section discusses effects of loading and environmental conditions on deformation and fracture of adhesive-bonded joints. The following subjects are discussed:

1) Effect of strain rate.
2) Effect of temperature.
3) Effect of environment.

1. Effect of Strain Rate

Effects of strain rate on mechanical properties of epoxy adhesives have been studied by Wegman, et al.[81, 82] Wegman made tensile tests on low-carbon steel rods bonded with epoxy resin. The time of failure ranged from six milliseconds to five minutes, with test temperatures ranging from -54° to 90°C (-65° to 201°F).

The adhesive tested exhibited greater resistance to rapidly applied stresses than to more gradually applied stresses. The adhesives were also shown to lose strength with increasing test temperature, whether tested rapidly or slowly.

Within a range of a high-temperature second-order transition point and a low-temperature second-order transition point, the test data fit an exponential equation as follows:[82]

$$S = Ae^{\frac{E}{RT}} , \qquad (33)$$

where S is the stress in the joint at failure, and the other terms have their usual meaning. Energies calculated from this expression are lower for fast than for slower rates of testing.

It was also shown that there is little change in bond strength until time to failure is below 100 milliseconds. Plots of stress versus 1/T for a series of test times show a decided discontinuity at 1/T = 0.0039 or -16°C.

2. Effect of Temperature

Effects of temperature on mechanical properties of adhesives have been studied to some extent. Several helpful review articles have appeared dealing with this subject.[83, 84, 85, 86]

Figure 28 shows temperature dependence of short-time tensile-shear strength of various adhesives.[84, 86] Strengths of adhesives, like strengths of metals, decrease with increasing temperature.

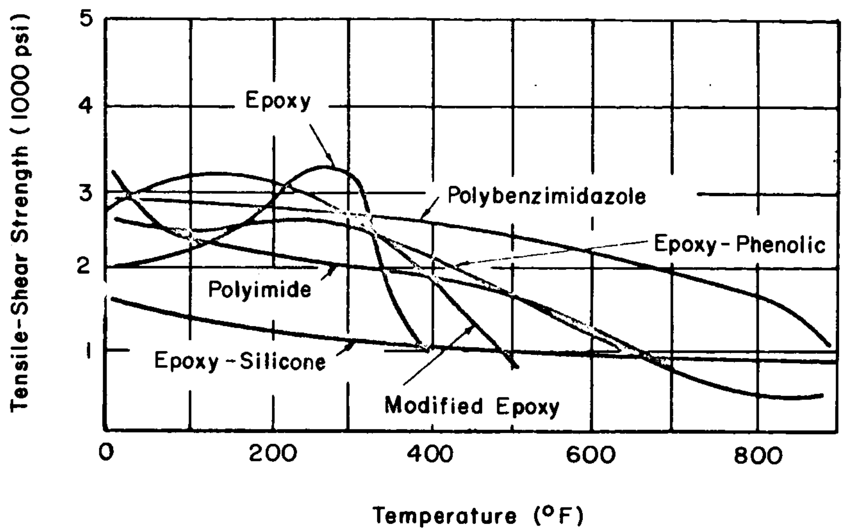

Figure 28. Temperature Dependence of Short-Time Tensile-Shear Strengths of Various Classes of Adhesives (Kausen)[84]

Figure 29 shows effects of time at temperature on tensile-shear strengths of joints bonded with various adhesives.[84, 86] At elevated temperatures, strengths of adhesive-bonded joints generally decrease with time.

Kausen's survey[84] includes strengths of adhesives at low temperature. Figure 30 summarizes tensile-shear strengths of various adhesive types. Different adhesives showed different temperature effects. At temperatures near room temperature, some adhesives show increasing strength with decreasing temperature. At very low temperatures, however, most adhesives have low strengths.

3. Effects of Environment

The performance of adhesive-bonded aluminum lap joints when exposed for long periods to various environments was studied by Olson, et al.[87] They studied joints in both stressed and unstressed states, using Florida and Panama sites for the exposure. They found that the adhesives lost considerable strength in outdoor exposure, and

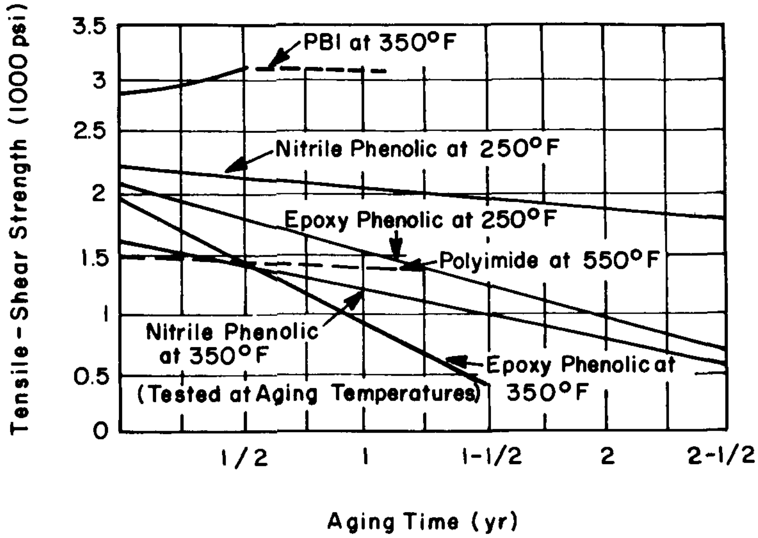

Figure 29. Effect of Time at Temperature on Tensile-Shear Strengths of Joints Bonded with Various Adhesives (Kausen)[84]

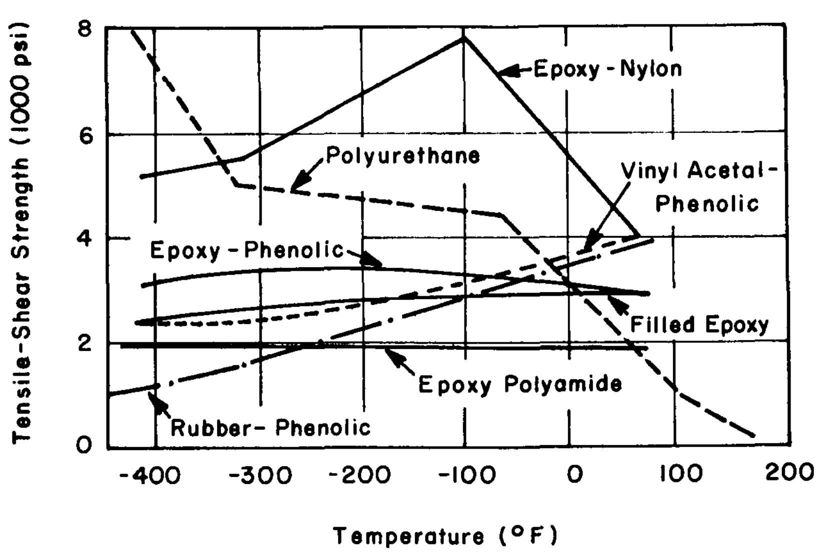

Figure 30. Tensile-Shear Strengths of Adhesive Systems for Cryogenic Service as a Function of Temperature (Kausen)[84]

in general the Florida site was more detrimental than the Panama site. They also found that exposure in the stressed condition accelerated the effect of the environment.

Sharpe[88] used this final conclusion as a basis for studies on the effects of humidity on the strength of adhesive joints. Earlier tests have shown that certain epoxy adhesives absorb large quantities of moisture and, in this wet condition, show a marked decrease in strength. However, in these tests the joints have been submerged in water in an unstressed condition, removed, and then stressed to failure. This does not take into account what will more likely occur in a practical situation - stress and moisture exposure being simultaneously present for a long period. Sharpe felt that this simultaneous effect was crucial when testing adhesive joints for aging or durability. His work took this into account, and the results indicated that moisture affects the ability of a joint to bear prolonged mechanical stress.

He subjected adhesive joints to shear stress in a high-humidity environment with mildly elevated temperature. The stress needed for short-term failure under these conditions was much less than for conditions of low humidity and identical temperature. This was true for all adhesives that Sharpe examined, although there was wide variation among adhesives in the stress required for failure.

From these tests, Sharpe drew the following conclusions:

1) The ability of an adhesive joint to bear prolonged stress is decreased markedly by moisture.
2) The failure of adhesive joints simultaneously subjected to stress, humidity, and mildly elevated temperature is not creep-induced. It is catastrophic. The mechanism of failure is unknown.
3) The significance of joint performance in the test in relation to performance of a bonded structure in a service environment is unknown. However, one is inclined to be more confident of an adhesive which survives for 100 days in the test than of one which survives for 10 days.
4) The test is very useful for determining the relative efficacy of various prebond surface treatments.

Yeager[89] recently studied the effects of extreme temperatures on adhesive systems, using commercial adhesives. The systems were exposed to simulated reentry heating, lunar orbiting, and heated space vacuum. They were then evaluated for strength at temperatures ranging from -320° to 3000°F. In the tests, substructure bonding to both solid ablators and to honeycomb were evaluated. Two commercial epoxy phenolic adhesive systems were evaluated for attachment of a filled core to a metal substructure. Evaluations were made for lap tensile shear strength and for flatwise tensile strength for steel-to-steel and filler-to-steel joints.

Steel-to-steel tensile shear strength was measured after a 30-minute exposure to various temperatures. All failures occurred cohesively within the adhesive. Each of the two systems mentioned above was exposed to a 14-day soak test at 250°F under 10^{-5} mm Hg. Tests were made at room temperature, and neither showed a reduction in bond strength. The steel-to-steel flatwise tensile strength comparisons after a 30-minute exposure to various temperatures showed the same results as above.

Section VIII. DESIGN AND FABRICATION PROBLEMS

1. Background

There are a number of problems regarding design and fabrication that affect the strength of adhesive-bonded metal structures. This section describes briefly design and fabrication problems related to fundamentals of deformation and fracture of adhesive-bonded joints. They will be discussed under major categories as follows:

1) Empirical methods of joint design.
2) Effect of metal surface on the strength of adhesive-bonded joints.
3) Effects of setting of the adhesives and residual stresses on the strength of joints.

2. Empirical Methods of Joint Design

With an empirical method of design, we hope to provide a simple relationship between experimental data and design criteria.[13] This relationship may be based on simplifying more complex analyses, on experience with known, proven methods, or merely on engineering judgment. In lap-joint design, all of these approaches have been used to some extent.

The use of strength data from simple lap-joint tests would be an ideal method of joint design because the information is readily available. The best variable to use from such information would be that of average shear strength of the adhesive (τ_a). The adhesive usually acts as a shear-transfer medium in lap-joint structure, and this property is best given by shear strength.

The lap-joint strength $\tau_a = P/A$ can be expressed as a function of K, commonly called the joint factor, where K represents various forms of overlap length to adherend thickness ratio:[13]

$$\tau_a = f(K) \quad . \tag{34}$$

Table III lists formulas for the joint factor K proposed by different investigators.

Table III. Formulas for the Joint Factor, K, for a Lap Joint[13]

Investigator	K
DeBruyne[90]	$\sqrt{t_1}/L$
Sheridan and Merriman[91]	L/t_1
Tombach[92]	$A\left(L/\sqrt{t_1}\right)B$
Brown[93]	$A + B\left(\sqrt{t_1}/L\right)$
Brown[93]	$\sqrt{\frac{t_1 + t_2}{2}}\Big/L$

where L is overlap length, t_1 and t_2 are adherend thickness, and A and B are constants.

In using strength data for joint design, an engineer must decide whether it will be representative of data that might be expected from production assemblies. Criteria must be set up concerning the ranges of the joint factor that are acceptable for design purposes.

Houwink and DeBruyne[4] have related this empirical method to a more complex rational analysis. They started with Volkersen's result for a lap joint without bending,

$$\frac{\tau_m}{\tau_a} = \Delta \coth \Delta \tag{35}$$

where τ_m is maximum shear stress and τ_a is average shear stress.

$$\tau_a = \tau_m \cdot f(\Delta) \quad , \tag{36}$$

where (refer to Figure 4 for symbols)

$$\Delta^2 = \frac{G_a L^2}{E_1 t_a t_1} \quad . \tag{37}$$

For a series of joints then bonded with the same adhesive, Δ is a function of L/t_1, and therefore

$$\tau_a = f\,(L/t_1) \quad , \tag{38}$$

which is the same result obtained previously.

A major advantage of the empirical method of design is that the lap-joint tests are simple and economical to make. Thus far, it has been a workable method. However, there are several disadvantages of the method:[13]

1) A large number of lap-joint tests are required to develop the curves of $\tau_a = f(L/t_1)$.
2) The curve, when obtained, is good only for a specific set of conditions and a specific test temperature. Any change, for example in surface treatment or in the temperatures at which the structure would be used, would require new tests. Elastic properties should not be as greatly affected by these factors as strength properties. Still, this disadvantage will be true to some extent for other tests, such as the torsion cylinder.
3) The method provides no information on properties of the joint up to and just prior to failure. It is based solely on inelastic joint properties.
4) Compared to what the joint can actually withstand in a structure, the information is probably very conservative. This is because the adhesive in a lap joint is subject to a more complex stress field with high normal stresses present. This causes failure at a lower level than in a structure where the joint has been designed to minimize the peel forces.

3. Effect of Metal Surface on the Strength of Adhesive-Bonded Joints

Surface preparation of the adherends can have a substantial effect on the strength of an adhesive-bonded joint. There have been several investigations on this subject. Matting and Ulmar[94] used three different adhesives in measuring shear strength of an aluminum-copper-magnesium alloy joint. From these studies, they rated different methods of surface preparation as follows: degreasing 1, polishing 4, grinding 5.5, acid pickling 6, and grinding and pickling 7. Higher numbers indicate higher strengths. The concluded that even though a surface is degreased, it must also be chemically or mechanically activated if maximum strength is to be attained. They found similar differences in bond quality for steel surfaces, but the surfaces that were only degreased were less inferior than with the alloy.

Levine, et al.,[95] studied surface treatment by comparing the contact angle of an epoxy resin on steel panels with the tensile shear strength of the joint. They were able to show the efficiency of various solvents and of sonic treatments through decrease of the apparent contact angle and an associated increase in bond strength. Their work involved use of solvents, mechanical treatments, and chemical treatments. Grit blasting was a mechanical means shown to be quite effective by this study. Other references of interest in this area include Salmon, who analyzed the balance between chemical and mechanical factors in the surface treatment of steel, and Schliekelmann.[96]

Schonhorn and Sharpe[97] correlated the rates of setting, wetting, and spreading in regard to adhesive-bond strength. They distinguished three conditions:

1) At low temperatures, where the adhesive surface does not flow, maximum joint strength will be attained if the wetting equilibrium is reached before the adhesive resin starts to set.
2) Poor bonds will result if setting takes place before wetting is completed.
3) High bond strength will result, regardless of the previous degree of wetting, if after-curing at high temperatures allows the adherend to become mobile enough to spread on the hardened adhesive.

Forest Products Laboratory[98,99,100] conducted tests on surface treatment of clad 24S-T3 aluminum alloy. The methods of treatment employed included vapor degreasing, meta-silicate degreasing, abrading, and various acid treatments. The method found to result in best bond strength used a sulfuric acid, sodium dichromate solution. The alloy was prepared by wiping with a solvent, immersing for 10 minutes in a 140° to 150°F solution of 10 parts sulfuric acid, 1 part sodium dichromate, and 30 parts water, rinsing, and drying. Joints prepared in this manner proved superior both in original strengths and after salt-water-spray exposure.

There are a large number of reports concerning preparation of other metals, such as bare aluminum alloys, magnesium, stainless and alloy steels, and titanium.[98,99,100,101,102,103,104,105,106,107,108] Comparative rankings of effectiveness of different surface treatments obtained by different investigators are often inconsistent.

4. Effects of Setting of the Adhesives and Residual Stresses on the Strength of Joints

In the adhesive-bonding process, an adhesive undergoes a transition from a soft and viscous state to a fixed or hardened state by chemical or physical actions, such as condensation, polymerization, oxidation, vulcanization, gelation, hydration, or evaporation of volatile constituents. This group of phenomena is called setting or curing. Physical and mechanical properties change during setting. Maximum strength is usually obtained after complete setting.

All adhesives shrink as they set. This may be due to cooling, to loss of solvent, or to chemical changes, depending on the type of adhesive and application. The differential contractions between the adhesive and the adherend induces residual stresses in the adhesive-bonded joint. In most cases, high tensile stresses in the direction parallel to the joint are produced in the adhesive. Aleck[109] calculated the stress distribution at the interface due to thermal contraction.[10] The important conclusion was that the greatest stresses occur at the ends of the interface. Residual stresses in the adhesive-bonded joints have been analyzed approximately by Dietz, et al.,[110] for thin, rigid adhesive lines, and by DeBruyne and Mylonas[4] for deformable adhesive layers of finite thickness.

High tensile residual stresses in the adhesive can affect the strength of the joint when certain conditions are present. Extensive research has been performed during the last decade on the fracture strength of fusion-welded steel structures.[111, 112, 113] It has been found that:

1) The effect of residual stresses is negligible when the material is ductile; fracture occurs after considerable plastic deformation.
2) The effect of residual stresses can be significant when the material is brittle; fracture occurs with little plastic deformation.

When the material is brittle and a notch is located in an area containing high tensile residual stresses, fracture can initiate from the notch and propagate even when the applied stress is considerably lower than the yield strength of the material. The low-applied-stress fracture of fusion-welded steel specimens has been demonstrated by several investigators, including Wells,[111, 114] Kihara and Masubuchi,[115] and Hall, et al.[116, 117, 118]

Very limited attention has been given to the effect of residual stresses on the fracture strength of adhesive-bonded joints. On the basis of the information obtained on fusion-welded specimens, the effect of residual stresses on the strength of adhesive-bonded joints will be significant only when the adhesive is brittle. Residual stresses may be an important factor for reducing the strength of the adhesive-bonded joint at cryogenic temperatures. More study is needed on this subject.

PRECEDING PAGE BLANK NOT FILMED.

Chapter 2

MECHANISMS OF DEFORMATION OF METAL-ADHESIVE INTERFACES

Section I. INTRODUCTION AND BACKGROUND

One of the possible failure modes of adhesive-bonded joints is by gross plastic deformation of the adherends. Such failures have been observed in lap-shear specimens composed of relatively weak adherends, such as annealed aluminum or titanium, bonded with some of the stronger modified epoxy adhesives.[85] When failures by adherend deformation are encountered, investigators have simply avoided them by using thicker-than-standard adherend strips or by decreasing the overlap of the joint from the standard one-half-inch value. Similar practice has been followed with respect to design of joints intended for service. Joint dimensions have been adjusted to result in failure in the bond line.

Apparently no attention has been paid to the occurrence of adherend plastic flow, to its influence on joint strength, or to the influence of the adhesive on the onset of such flow. However, it is likely that at least small amounts of adherend plastic flow can occur in adhesive-bonded joints, especially at edges and corners of the bonded area. It has been pointed out previously in this report that these edges and corners are regions of stress concentration. A great body of literature exists on the theoretical and experimentally observed details of plastic deformation in solids. A portion of this literature is devoted to the influences of free surfaces and interfaces on plastic flow. None of the literature deals specifically with films of adhesives, but it is probable that some of the known principles set out in the literature can be applied to the case of metals coated with adhesives.

Therefore, a discussion of the mechanisms of plastic deformation of solids will be presented in this section of the report, beginning with some of the properties of dislocations. It is recognized that very little of the theoretical work on dislocations in metals[119,120,121] has a direct bearing on adhesive-bonded joints. Nevertheless, a brief discussion of some aspects is included here for perspective.

1. Plastic Deformation and Dislocations

The basic unit of plastic flow in crystalline solids is the structural defect known as dislocation. Plastic flow by motion of dislocations has been amply demonstrated not only in metals, but also in ionic crystals and in crystalline ceramics. Dislocations are line defects within single-crystal lattices. They can extend along different paths through the crystal, though some paths are preferred, but they cannot end within a crystal. In polycrystalline materials, the crystal boundaries usually serve to limit and confine dislocations. It is virtually impossible to create crystalline materials entirely free from dislocations, though carefully grown and well annealed crystals may have remarkably few - as few as 100 dislocation lines passing through any given square-centimeter cross section.

On application of mechanical stress to a crystal, there is little or no motion of the preexistent dislocations in the elastic stress region. At a stress in the neighborhood of the engineering yield stress, however, two things happen: there may be a significant amount of motion of existing dislocations, and there will certainly be a generation of large numbers of fresh dislocations from sources within or at the boundaries of the individual crystals in the solid. It is this dislocation multiplication that gives rise to microscopic and macroscopic slip. The interferences and interactions among the dislocations produced results in the well-known phenomenon of strain hardening. Passage of a single dislocation through a crystal will produce an amount of slip in the crystal equal to the length of the Burgers vector of the dislocation. This length is usually of the same order as the side length of the crystal unit cell, or about three to four angstrom units (three to four x 10^{-8} centimeters). Thus, it can be seen that motion of enormous numbers of dislocations is required to produce large amounts of plastic flow. Dislocation densities up to 10^{12} per square centimeter are common in heavily deformed metals. With such high concentrations of dislocations, their spatial arrangements are hopelessly complex, and it is no longer possible to make observations of the behavior of individual dislocations.

During at least the early stages of plastic flow, before the dislocation density has increased more than a few orders of magnitude, motion of dislocations in response to an external applied stress is along fairly well defined crystallographic planes and in definite crystallographic directions. It has already been pointed out that a certain value of applied stress is required to initiate appreciable dislocation motion. This stress is known as critical shear stress and can be determined for any slip plane relative to the applied external stress direction.

In a polycrystal, unless a strong preferred orientation texture is present, it follows that from random variation certain crystals in the mass will be oriented so as to have higher resolved shear stresses on their slip planes than exist in surrounding crystals. Slip will tend to take place first in these isolated, favorably oriented crystals. Only as the applied stress is further increased will the deformation become general throughout the solid.

2. Boundaries and Dislocations

The detailed structure of the general, or high-angle, grain boundary between crystals is not known. It is probable that there is no single structure, but that crystals simply fit together as best they may. Grain boundaries have higher energy than the crystals themselves and act as both sources and sinks for dislocations.

When crystals do not differ in orientation by more than about 17 degrees, a simpler boundary can exist between them, known as a low-angle boundary. In its simplest form, a low-angle boundary consists either of a parallel array of evenly spaced edge dislocations (a tilt boundary) or of a square array of screw dislocations (a twist boundary). If both tilt and twist components exist between the lattices of the crystals, or if the boundary is curved, the dislocation array becomes more complex. The boundary structure is still simple compared with a high-angle boundary, however.

So far, the discussion has assumed that the crystals on either side of the boundary are composed of the same material. If the boundary in question is one between, say, a precipitate particle and its matrix, or between a metal and its oxide, mismatching, even between parallel crystal lattices, will exist. This type of mismatching is due solely to the fact that crystal structures, and hence lattice parameters, are different on either side of the boundary.

The dislocation arrays in low-angle boundaries and between boundaries of different crystalline phases have been studied by thin-film electron microscopy techniques.[122, 123, 124, 125, 126]

The adhesive-adherend interface is also a boundary between dissimilar materials. However, the adhesives as a class fail to meet the requirements of crystallinity that is necessary for the existence of boundary dislocation arrays at the interface. Although some plastics that could conceivably be used as adhesives possess a limited degree of crystallinity, it is probably safe to assume that adhesives are amorphous. Mechanisms for the influence of adhesive films on plastic flow of metal adherends must not assume the existence of boundary dislocation arrays.

3. Dislocation Sources

Sources for the large numbers of dislocations necessary for plastic flow can at least be grain boundaries, inclusions, vacancy clusters, precipitate particles, surface irregularities, and dislocations themselves (the Frank-Read source). An activation energy is associated with the operation of any of these sources. This energy is usually supplied by the external applied stress. Sources of dislocations can be located at or beneath the surface of the crystal. Fisher[127] has shown that for a Frank-Read type of source, whose activation energy is a function of the source length, a surface source can operate at one-half the applied stress required to activate an interior source of the same length. Thus, surface sources, if they are not blocked by the action of films, will generally tend to be the origin of the first slip taking place on the application of increasing stress.

4. Dislocation Pileup

In addition to blocking of surface dislocation sources, films and layers of dissimilar materials can also act to block the escape of moving dislocations from within the crystal. When dislocations are blocked, pileups of dislocations are formed on the active slip planes.

Section II. EFFECTS OF SURFACE FILMS ON STRENGTH

Presence of surface films will generally result in increased strength in metals. The observed strengthening is often greater than can be accounted for solely on the basis of the strength of the film itself. It is therefore reasoned that one or both of the previously-mentioned mechanisms, suppression of surface dislocation sources or blocking of emerging dislocations, must be operative. The strengthening effects of films may appear as a decreased amount of slip and an increased rate of work hardening, or there may also be an increased yield strength. In some cases, yield strength is scarcely affected by the presence of a film.[128] It should be noted that obtaining a film-free specimen and preventing formation of at least an adsorbed moisture, oxygen, or oxide film during testing presents serious experimental difficulties. Films form in fractions of a second at atmospheric pressure.

Kramer and Demer[129] have summarized the effects of environment on the mechanical properties of metals. In categorizing the literature, they recognized two classes of films: (1) oxide and metal films and (2) surface-active agents and electrolytes.

Adhesives fall into the second category, since they are subject to the same physico-chemical laws of surface wetting as surface-active agents. The adhesive joint, however, is seldom directly between the adhesive and the metal adherend. The cleaning procedures used to prepare the adherend surface leave films interposed between the metal and the adhesive. The compositions of these films may be complex, since the surface conditioning solutions often consist of combinations of chlorides, nitrates, fluorides, phosphates, or chromates. Inorganic films such as these would behave similarly to Kramer and Demer's first category - oxide and metal films.

1. Oxide and Metal Films

The strengthening effect of oxide films on metal crystals was first noted by Roscoe for cadmium in 1934 and has become known as the Roscoe effect.[130] Roscoe attempted to explain the effect in terms of healing of surface cracks by the films, an explanation that had been previously advanced by Joffe[131] to account for the strengthening of rock salt immersed in water. The crack healing mechanism for metal crystals is today considered to be much less likely than the mechanisms involving dislocations. The reader is referred to the comprehensive discussion by Kramer and Demer, which includes the effects of oxide and metal films on yield point, plastic deformation by slip and twinning, microscopic features of deformation, fracture, internal friction, creep, and fatigue. Although most of the data presented are for single crystals, some results are reported for polycrystals.

a. Dislocation Theory

Takamura,[132] studying oxide films on aluminum single crystals, noted a tendency for the crystals to twist as well as to extend in the tension direction when pulled. The twisting effect, which would have been overlooked if the test equipment had not had a rotational degree of freedom, began at stresses much below the yield stress. Takamura attributed the twisting to fine slip taking place even in the so-called elastic region of the specimens, and hypothesized that the dislocations were being held up at the surface by the presence of an oxide film.

Fleischer and Chalmers,[133] in their investigation of size effects in deformation of aluminum, calculated that, to explain some of their results, the strength of the oxide film had to be approximately equal to the theoretical strength of a perfect solid.

Head[134] has suggested that, for a film to interfere effectively with the motion of dislocations, the film must have a shear modulus higher than that of the crystal. The shear modulus of aluminum oxide is higher than that of aluminum, which leads to the prediction that aluminum oxide films should be effective in restraining motion of dislocations near the surface. Experimentally, this appears to be the case, since Makin and Andrade[135] have reported a significant size effect on strength of aluminum crystals coated with oxide films. In the case of copper, the oxides of which have lower shear moduli than copper itself, Suzuki, Ikeda, and Takeuchi[136] did not find a size effect attributable to the presence of the films.

b. Critical Shear Stress

Rosi,[137] working with silver-plated copper crystals, found that the critical shear stress for the onset of plastic flow was not appreciably increased by the silver unless the specimen had previously been given a thermal treatment to diffuse silver into the surface. This observation is interpreted as meaning that the dislocation sources near the surface are suppressed by presence of the foreign silver atoms in the copper lattice.

Adams[138] found that he could induce a yield point in copper crystals that had been coated with zinc, prestrained slightly, and diffusion annealed. The yield point was observed only at intermediate zinc levels. Neither pure copper crystals nor highly zincified crystals showed a yield point. The explanation proposed is that plastic flow in pure copper initiates at easily-activated surface sources. In heavily zincified crystals, these sources are completely blocked, and flow is initiated at sources within the crystal. At intermediate levels of zincification, it is proposed that the surface sources are only partially blocked, so that plastic flow still initiates from them, but at higher stresses than in pure copper, and with a yield point.

c. Stress-Strain Curve

Takamura, et al.,[132] observed that the strengthening effects of oxide films on aluminum crystals persisted throughout the stress-strain curve. They found, however, that the strengthening effect of a thin (100 A) film was greater than that of a thicker (500 A) film.

Garstone, Honeycombe, and Greetham[139] found that nickel-chromium plating of copper single crystals eliminated the Stage I, or easy glide, portion of the stress-strain curve. Strain hardening began immediately after yielding. Jemian[1] found a similar effect in chromium-plated and epoxy-coated specimens of OFHC copper having a bamboo structure. He also reported an increase in ultimate tensile strength in both cases. Rosi[137] found that his silver-plated copper crystals, as compared to a nitric acid-etched crystal, showed no change in the shape of the stress-strain curve. When the plated crystals were diffused, not only was the yield stress increased as previously noted, but an easy glide region appeared in the stress-strain curve. Appearance of the easy glide region is consistent with the behavior of copper when alloyed in bulk with silver. The similar behavior when silver was present only in the region near the crystal surface underscores the importance of surfaces in determining plastic flow behavior of metals. Chalmers and Davis[140] were able to show that a substructure of low-angle boundaries, formed after straining and annealing aluminum crystals, consisted of dislocations of sign such that they must have come from the crystal surface.

d. Creep

Oxide layers have been shown by Sweetland and Parker[141] to increase the creep strengths of polycrystalline copper and aluminum.

e. Elastic Aftereffect

Cochardt[142] has studied the aftereffects of straining in polycrystalline aluminum and copper wires. The wires were first strained two percent in torsion at room temperature under a helium atmosphere. Their room temperature strain recovery was observed to be of the normal sort observed with the elastic aftereffect, and consisted of a gradual decrease of torsional strain with time. Cochardt then increased the ambient temperatures of the specimens to within the 300° to 700°C range. Aluminum specimens continued to untwist, which was interpreted as being the result of continued dissipation of dislocation arrays piled up behind the relatively strong oxide layer on aluminum. Retwisting (the Barrett anomalous aftereffect) was observed in the copper, which can be explained on the supposition that, instead of dissipating back into the crystals by reverse slip and climb, the dislocation pileups disappear by penetrating the oxide layer, which is relatively weak in the case of copper, and which is further weakened by the increased temperature.

Jemian and Law,[143] in as-yet unpublished results, have observed retwisting of copper wires upon removal of a zinc coating. This observation is important, since Young's modulus for zinc is lower than that of copper. Thus, according to Head,[134] zinc should not be effective in restraining dislocations at a copper-zinc coating interface.

2. Surface-Active Agents and Electrolytes

Surface-active agents, often called surfactants, are polar organic compounds whose molecular properties cause them to be strongly adsorbed on solid surfaces, including metals. The adsorption tendency results from the presence of certain specific atom groups in the surfactant molecule. These active groups are the attachment points of the molecules to the surface. In some cases, the surface will not strongly adsorb until some metal oxide has been formed or unless some water is present. In other cases, the metal surface must be microscopically clean and chemically active for the adsorption to occur. Kramer has related the adsorption of surfactants on clean surfaces to the emission of exo-electrons known to occur from freshly abraded metal surfaces.[144, 145] Kramer, having invariably detected the presence of soaps of the adsorbant metals in the aqueous solutions surrounding the metals, favors a chemisorption mechanism over physical adsorption. Whatever the mechanism, the adsorption process is one involving a decrease in surface-free energy and follows the usual sort of thermodynamic equations describing wetting phenomena. The mathematics is reviewed by Kramer and Demer[129] and will not be restated here.

Compared with the thicknesses of oxide films, surfactant layers are relatively thin, being limited to one or two molecules thick. The observed rates of formation of metal soap monolayers are often of the order of hours, much slower than for formation of oxide films in air.

Much of the fundamental work on the effect of surface-active agents on mechanical properties of metals has been done by Rehbinder and his co-workers. The increase in creep rate that occurs in both nonmetals and metals in the presence of such materials as straight-chain aliphatic acids is known as the Rehbinder effect. It is characteristic of the Rehbinder effect that, as the concentration of the acid in the nonaqueous solvent surrounding the loaded specimen is increased, the measured creep rate passes through a maximum value. Both the maximum creep rate increase and the surfactant concentration at which it occurs are different for different surfactants. The change in creep rate may be as high as 200 percent, and creep rate maxima occur at surfactant concentrations between 0.01 and 1 mole per liter.[146] Kramer has given an up-to-date explanation of the Rehbinder effect as being a sort of corrosion of the metal surface to form metal salts (soaps) of the organic acid surfactants. At low surfactant concentrations, soaps are rapidly formed, but there are relatively few acid molecules present, so the metal removal rate is low. If the metal removal rate is low, the removal rate of dislocation pileups near the surface will also be low. As the surfactant concentration is increased, the removal rate of metal and surface dislocation pileups will increase. The increase will show up as an increase in creep rate. With further increase in surfactant concentration, however, the solution boundary layer will quickly become saturated with soap and will become the rate-limiting step. Adsorption of the surfactant molecules will also increase with increasing concentration and will act to block an increasing fraction of the surface from the saponification reaction. Therefore, there will be a decrease in creep rate at high surfactant concentrations, although the creep rate will always be higher than specimens creep tested without the presence of surfactants.

Some investigations have been conducted of the effects of relatively dilute aqueous electrolytes on the shape of the stress-strain curve. These are discussed by Kramer and Demer, but are not included here because it is difficult to see any relationship between this work and the effects of films of organic adhesives on metal properties.

3. Polymer Films

Only two reported investigations were found in which the effects of polymer films on the strength of metal crystals have been studied. These were the work of Metzger and Read[147] and Jemian.[1, 2, 3] Personal contacts with Professors Metzger and Gilman (Professor Read is deceased), who are intimately acquainted with the current worldwide activity in this field, failed to disclose any additional published information.

Metzger and Read's investigation was performed using cadmium single crystals. They used etched, plastic-coated, and anodized surfaces. The mechanical property observed was the creep rate as measured in a constant-stress creep machine. The plastic coatings were applied by dipping and withdrawal prior to testing, however. Thickness of the plastic coatings was regulated by controlling the concentration of the dissolved plastic.

The effects of two plastics were studied - Formvar and Vulcalock. Formvar is a trade name for a series of polyvinyl-methylal resins. Vulcalock is a modified isomerized rubber type of cement manufactured by the B. F. Goodrich Company and intended for use as a rubber-to-metal adhesive.

Two cadium crystals were coated, one (Specimen D4-1) being oriented for easy glide and the other (Specimen F1-2) being oriented with the basal plane seven degrees from the direction of stress application. Basal slip would be difficult to initiate in Specimen F1-2. Table IV gives Metzger and Read's results for different film thicknesses. Measurable strengthening effects were found for films thicker than 700 A. The results of the analysis show that when the strengthening effect of the film (column headed "Equivalent Shear Resistance of Film") is compared with known shear strengths of the film materials in bulk (column headed "Bulk Shear Strength of Film Material"), it appears that the strengthening of the crystals, expressed as the initial increase in critical shear stress, by the films can be accounted for solely by the load-carrying contribution of the films. The films did not act to impede dislocation motion in the cadmium crystals. Neither did they result in a Rehbinder effect, with its loss of strength.

The extent to which Formvar and Vulcalock are representative of high-performance adhesive systems is not known, and the general applicability of Metzger and Read's findings cannot be assessed. Jemian's results[1] on the effect of epoxy coatings on strength of bamboo-structure copper wire specimens show elimination of easy glide and an increase

Table IV. Effect of Adherent Plastic Films on the Creep of Cadmium Crystals

Specimen	Film	Orientation χ (deg)	Shear-Stress Equivalent, $\Delta\tau_f$ (G/Mm^2)	Shear-Stress Equivalent (per 100 A)	Equivalent Shear Resistance of Film, S_f (Kg/Mm^2)	Bulk Shear Strength of Film Material (Kg/Mm^2)
D4-1	700 A Formvar	28[a]	0.54	0.077	2.0	3-4[c]
		28[b]	0.86	0.123	3.0	3-4[c]
	3700 A Vulcalock	26	0.61	0.016	0.38	0.4-0.7[d]
F1-2	700 A Formvar	7	0.21	0.030	0.9	3-4[c]
	1000 A Formvar	7	0.28	0.028	0.9	3-4[c]

[a] Test No. 2.

[b] Test No. 4.

[c] As measured with a punch-type jig on a 0.6-mm film laid down from solution.

[d] As reported by the manufacturer.

in ultimate tensile strength due to the epoxy. The amount of the increase was smaller, the longer the number of grains per inch in the copper (Figure 31). Jemian also reported discontinuous stress-strain curves believed to result from penetration of piled up dislocations through the copper-epoxy interface, to breaking of the epoxy from the copper, and to fracture of the epoxy film. Presence of the epoxy coating also changed the character of the observed slip traces from uniform fine slip to coarser, irregular slip.

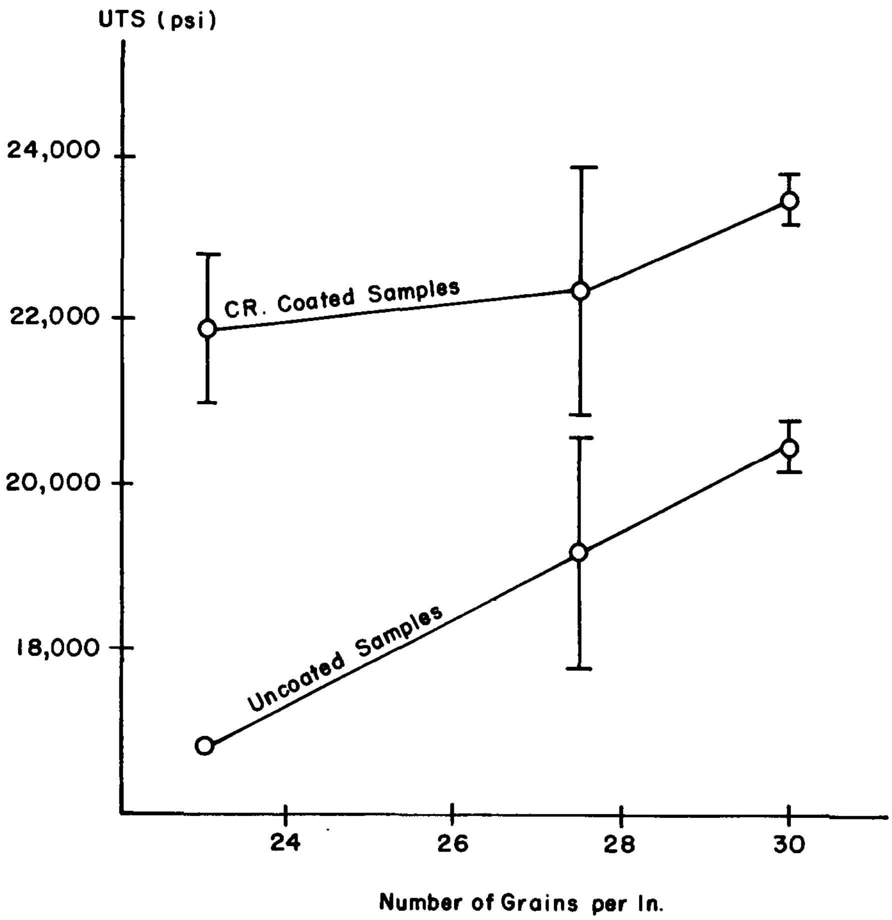

Figure 31. Effect of Grain Size on Properties of Wire (Jemian)[1]

Section III. SUMMARY OF MECHANISMS OF DEFORMATION OF METAL-ADHESIVE INTERFACES

In summary, solid films generally increase the mechanical properties of yield strength, strain hardening coefficient, creep strength, and fatigue strength of single crystal and polycrystalline metals. The amount of increase observed depends on the relative shear moduli and strengths of the metal and the film. Weak, inert organic films improve tensile properties only by an amount equal to the mechanical strength of the film, so far as is known. Intimately bonded oxide films may result in strengthening effects out of proportion to film thickness.

Surface-active agents tend to decrease mechanical properties of the underlying metals.

Electrolytes may either increase or decrease the strengths of metals. Most work with electrolytes has been done with reference to creep strengths.

Very little study has been made of the effects on metal strength of organic materials primarily intended as adhesives, so far as is shown.[1]

PRECEDING PAGE BLANK NOT FILMED.

Chapter 3

CONCLUSIONS AND RECOMMENDATIONS

Section I. CONCLUSIONS

There is presently a large amount of data available on mechanical properties of various types of adhesive-bonded joints. However, only limited information is available on fundamentals of deformation and fracture of the joints.

Today, composite materials are called upon to provide properties unattainable in the constituents themselves. Simple materials, acting alone, simply cannot meet the diverse and severe demands placed on them by today's advanced technologies. The various composites that replace them are often fabricated using a variety of adhesives. The adhesive-bonded joints are subjected to a wide variety of loading and environmental conditions. Because of the complexity, the scientific approach to the problem of deformation and fracture information would be an efficient way to improve properties of adhesive-bonded joints. On the basis of recent advances in various areas of science and technology, it is believed that such an approach would yield useful information. Some of the areas in which such information could be obtained are discussed in the following section.

Section II. RECOMMENDATIONS FOR FUTURE RESEARCH

Research in the following areas would lead to better understanding of fundamentals of deformation and fracture of adhesive-bonded joints.

1. Elastic Stress Distributions in Adhesive-Bonded Joints

When the magnitude of the external load is relatively low, an adhesive-bonded joint deforms elastically. There has been some analysis of elastic stress distribution in adhesive-bonded joints, as described in this report. However, due to the restriction of hand calculation, most of the analyses conducted so far have been limited to simple cases. In the analysis by Goland and Reissner, for example, studies were made on two extreme cases; (1) joints with inflexible adhesive layers, and (2) those with flexible adhesive layers. Modern computers should make it possible to extend the analysis to more general cases. However, the demand for such extension would be less than in other areas where virtually no fundamental studies have been made.

2. Onset of Plastic Deformation

When the magnitude of the external load is increased, a portion of an adhesive-bonded joint will undergo plastic deformation. The plastic deformation first occurs at the edge of the joint where stress concentrations take place. As the magnitude of the external load is increased, the amount of plastic deformation increases and the plastic zone expands; however, the gross deformation of the joint does not increase significantly, because a large portion of the joint still remains elastic. No mathematical analysis has been made of elasto-plastic stress distribution in adhesive-bonded joints. On the basis of recent development of mathematical theory of plasticity, the analysis of onset of plastic deformation in adhesive-bonded joints can be advanced. This problem is very important to better understanding of mechanisms of fracture in adhesive-bonded joints.

3. Plastic Deformation of Adhesive-Bonded Joints After General Yielding

When the external load reaches a certain value, the plastic zone extends over the entire width of the joint, resulting in general yielding. An exact analysis of stress and strain distributions beyond general yielding would be very difficult, because strains can no longer be considered infinitesimal.

4. Inelastic Deformation Under Sustained Loading

When the external load is applied for an extended period, deformation of an adhesive-bonded joint increases due to inelastic deformation of adhesive and/or adherends. The inelastic deformation becomes more predominant at higher temperatures. However, because stress and strains are functions of time as well as locations in the joint, mathematical analysis of the inelastic deformation would be very difficult.

5. Experimental Analyses of Stresses in Adhesive-Bonded Joints

It is important to determine experimentally the distribution of stresses in adhesive-bonded joints. The following techniques that have been developed rather recently would be useful for studying stress distributions in adhesive-bonded joints:

1) Photoelastic coating technique.
2) Three-dimensional photoelasticity.

A unique advantage of the photoelastic coating technique is that stress measurements can be made on actual adhesive-bonded joints instead of on a photoelastic model. This technique has been applied to a limited extent, but more studies are needed on this subject.

The three-dimensional photoelasticity technique allows study of stress distributions inside the joint and could be quite useful for future research.

6. Micromechanisms of Fracture of Adhesive-Bonded Joints

Only limited studies have been made on micromechanisms of fracture of adhesive-bonded joints. Electron microscopes would be useful for studying micromechanisms of fracture of adhesive-bonded joints.

7. Atomic Mechanisms of Fracture of Adhesive-Bonded Joints

To understand fundamental mechanisms of fracture, it is very important to place the mechanisms on an atomic scale. This will be very difficult with adhesive-bonded joints, but should be attempted. During the last few decades, extensive studies have been made of atomic mechanisms of fracture of metals and other materials which have rather regular atomic structures. Since organic adhesives do not have regular atomic structures, basic studies need to be made first to determine what models should be used.

8. Effects of Loading and Environmental Conditions on Deformation and Fracture of Adhesive-Bonded Joints

More fundamental studies, analytical or experimental, are needed on effects of loading conditions (such as impact and repeated loading) and environmental conditions (such as temperature, water, and other media) on deformation and fracture of adhesive-bonded joints.

9. Recommendation for Continuation of Literature Survey

Because technology is expanding rapidly and new knowledge is being gained throughout the world, surveys of fundamental subjects are very important. It is becoming more and more difficult for the engineer or scientist to keep up to date with new information in his field that can be useful in solving technical problems. Thus, it is recomcended that the survey of literature be continued to provide up-to-date information to those engaged in research in adhesives bonding and in application of adhesives bonding to various structures. This survey should cover both practical subjects and fundamental subjects such as those discussed in this report.

An important, logical extension of the present study would be a literature survey on fundamentals of deformation and fracture characteristics of adhesive-bonded structures. The present survey concerned such characteristics of adhesive-bonded joints as stress distribution and fracture strength. However, it did not cover such structural problems as: (1) onset and growth of plastic deformation, (2) fracture, (3) buckling, and (4) vibration characteristics of adhesive-bonded metal structures. During the last decade, considerable information has been gathered on the plastic-limit design concept and the fracture-safe design concept. The feasibility of applying such new concepts for the design of adhesive-bonded structures should also be surveyed.

LITERATURE CITED

1. School of Engineering, Auburn University, STUDY OF THE ONSET OF PERMANENT DEFORMATION IN STRUCTURALLY BONDED JOINTS by W. A. Jemian, September 1965, Report No. 1, U. S. Army Missile Command, Redstone Arsenal, Alabama (Unclassified).

2. School of Engineering, Auburn University, STUDY OF THE ONSET OF PERMANENT DEFORMATION IN STRUCTURALLY BONDED JOINTS by W. A. Jemian, April 1966, Report No. 3, U. S. Army Missile Command, Redstone Arsenal, Alabama (Unclassified).

3. School of Engineering, Auburn University, STUDY OF THE ONSET OF PERMANENT DEFORMATION IN STRUCTURALLY BONDED JOINTS by W. A. Jemian, January 1966, Report No. 2, U. S. Army Missile Command, Redstone Arsenal, Alabama (Unclassified).

4. N. A. DeBruyne and R. Houwink (editors), ADHESION AND ADHESIVES, Amsterdam, Elsevier, 1951.

5. STRUCTURAL ADHESIVES, London, Lange, Maxwell, and Springer, Ltd., 1951.

6. U. S. Naval Ordnance Laboratory, White Oak, Maryland, ADHESIVES HANDBOOK, PART I, ENGINEERING PRINCIPLES, by H. A. Perry, Jr., L. Hardis, H. E. Mathews, Jr., L. Briggs, E. W. Eagleson, and R. S. Fey, February 1952, NAVORD Report 2272 (Unclassified).

7. STRUCTURAL ADHESIVES FOR METALS AND SANDWICH CONSTRUCTION, U. S. Air Force, Aircraft Industries Association Conference, December 1952, Dayton, Ohio.

8. SAAB Aircraft, METAL BONDING PRACTICE AT SAAB by O. Ljungstrom, January 1955, Report KRP-O-L07 (Unclassified).

9. H. A. Perry, ADHESIVE BONDING OF REINFORCED PLASTICS, New York, McGraw-Hill, 1959.

10. N. K. Benson, THE MECHANICS OF ADHESIVE BONDING, Applied Mechanics Review, Vol. 14, No. 2, February 1961, pp. 83-87.

11. I. Sneddon, THE DISTRIBUTION OF STRESS IN ADHESIVE JOINTS, Chapter 9, Adhesives, New York, London, Oxford University Press, 1961.

12. N. E. DeBruyne, THE MEASUREMENT OF THE STRENGTH OF ADHESIVE AND COHESIVE JOINTS, Chapter 4, Adhesion and Cohesion, Amsterdam, Elsevier, 1962.

13. Forest Products Laboratory, U. S. Department of Agriculture, MECHANICS OF ADHESIVE BONDING LAP-TYPE JOINTS: SURVEY AND REVIEW, December 1964, Technical Documentary Report No. ML-TDR-64-298, for Air Force Materials Laboratory, Research and Technology Division, Air Force Systems Command, Wright-Patterson Air Force Base, Ohio (Unclassified).

14. J. L. Gardon, THE VARIABLES AND INTERPRETATION OF SOME DESTRUCTIVE COHESION AND ADHESION TESTS, Unpublished Book, Treatise on Adhesives and Adhesion, to be Published by Marcell Dekker, Inc. (Information Was Obtained Through Professor W. A. Jemian).

15. G. H. Dietz, COMPOSITE MATERIALS, American Society for Testing and Materials, Edgar Marburg Lecture, 1965.

16. I. Armovlevic, Z. ARCH. ING-WESEN., Hanover, 1909, p. 414.

17. P. Fillunger, OST. WOCHENZEITSCHRIFT RUN DEN OFFENTL BAUDIENST, 1919, p. 78.

18. O. Volkersen, LUFTFAHRTFORSCHUNG, Vol. 15, 1938, p. 41.

19. M. Goland and E. Reissner, STRESSES IN CEMENTED JOINTS, Journal of Applied Mechanics, Vol. 11, No. 1, 1944, pp. A17-A27.

20. NAT. LUCHTVAARTLABORATORIUM by F. J. Plantema, Amsterdam, 1949, Report M. 1181 (Unclassified).

21. U. S. Forest Products Laboratory, Madison, Wisconsin, STRESSES IN A LAP JOINT WITH ELASTIC ADHESIVE by R. E. Sherrer, 1957, Report 1864 (Unclassified).

22. R. W. Cornell, DETERMINATION OF STRESSES IN CEMENTED LAP JOINTS, Journal of Applied Mechanics, Vol. 20, No. 3, 1953, pp. 355-364.

23. Douglas Aircraft Company, Inc., Santa Monica, California, STRESS DISTRIBUTION IN THE ADHERENDS OF BONDED LAP JOINTS, PART II by K. F. Hahn, March 1961, Research Report SM 40010 (Unclassified).

24. Douglas Aircraft Company, Inc., Santa Monica, California, PHOTOSTRESS INVESTIGATION OF BONDED LAP JOINTS, PART II by K. F. Hahn, February 1961, Research Report SM 40001 (Unclassified)

25. D. D. Eley, ADHESION, London, New York, Oxford University Press, 1961.

26. R. F. Tylecote, SPOT WELDING, PART II (A PHOTOELASTIC INVESTIGATION ON THE STRESS DISTRIBUTION IN SPOT WELDS), Welding Journal, Vol. 20, 1941, pp. 359s-368s.

27. K. Ito, NOTE ON ADHESIVE STRENGTH TEST BY LAP JOINTS, Inst. Phys. Chem. Res., Tokyo, Scientific Paper 54, 1960, pp. 295-306.

28. K. F. Hahn and D. F. Fouser, METHODS FOR DETERMINING STRESS DISTRIBUTION IN ADHERENDS AND ADHESIVES, Journal of Applied Polymer Science, Vol. VI, No. 20, 1962, pp. 145-149.

29. O. Ljungstrom, Paper Read at Conference on Bonded Aircraft Structures at Aero Research Ltd., Duxford, Cambridge, England, May 1957.

30. THERMO MECHANICAL ANALYSIS OF STRUCTURAL JOINT STUDY by J. W. Lobbett and E. A. Ross, 1962, WADD TR 61-151 (Unclassified).

31. Douglas Aircraft Company, Inc., Santa Monica, California, RESEARCH AND THERMOMECHANICAL ANALYSIS OF BRAZED OR BONDED STRUCTURAL JOINTS by J. F. Goodwin, 1962, Contract No. AF 33(657)-8542 (Unclassified).

32. AERO RESEARCH TECHNICAL NOTE NO. 61 by N. A. DeBruyne, February 1948.

33. D. C. Drucker and R. T. Shield, BOUNDS ON MINIMUM WEIGHT DESIGN, Quarterly of Applied Mathematics, Vol. 15, July 1957, pp. 269-281.

34. NAT. LUCHRVAARTLABORATORIUM by A. Hartman, Amsterdam, 1948, Report M. 1275 (Unclassified).

35. G. Muller, DR. ING. THESIS, Technical University of Berlin-Charlottenburg, 1959.

36. Midwest Research Institute, THE STRESS OF DISTRIBUTION IN ADHESIVE JOINTS by J. L. Lubkin, September 1953, Final Report, Contract No. NOrd 13383 (Unclassified).

37. J. L. Lubkin and E. Reissner, ASME TRANS. Vol. 78, 1956, p. 1213.

38. E. G. Coker, AN OPTICAL DETERMINATION OF THE VARIATION OF STRESS IN A THIN RECTANGULAR PLATE SUBJECTED TO SHEAR, Proceedings Royal Society, London, Vol. 86, No. A587, 1912, pp. 291-319.

39. C. Mylonas, ON THE STRESS DISTRIBUTION IN GLUED JOINTS, Proceedings of 8th International Congress of Applied Mechanics, London, 1948, pp. 173-249.

40. C. Mylonas, EXPERIMENTS ON COMPOSITE MODELS WITH APPLICATION TO CEMENTED JOINTS, Proceedings of Society Experimental Stress Analysis, Vol. 12, 1954, pp. 129-142.

41. A. S. McLaren and I. MacInnes, THE INFLUENCE ON THE STRESS DISTRIBUTION IN AN ADHESIVE LAP JOINT OF BENDING OF THE ADHERING SHEETS, British Journal of Applied Physics, Vol. 9, 1958, pp. 72-77.

42. U. S. Forest Products Laboratory, PHOTOELASTIC ANALYSIS OF SHEAR STRESS DISTRIBUTION IN ADHESIVE-BONDED LAP JOINTS by D. Kutscha, July 1962, Report TP-122 (Unclassified).

43. U. S. Forest Products Laboratory, PHOTOELASTIC ANALYSIS OF SHEAR STRESS DISTRIBUTION IN LAP-TYPE JOINTS by D. Kutscha, June 1966, Order IPR-1964-8004(WEPS) (Unclassified).

44. E. N. Andrade, THE DISTRIBUTION OF SLIDE IN A RIGHT SIX-FACE SUBJECT TO PURE STRESS, Proceedings Royal Society, London, Vol. A 85, 1911, pp. 448-461.

45. Chrysler Corporation, JOINTS - LAP, EFFICIENCY, GRAPHICAL STUDY OF PHYSICAL FACTORS by C. C. Jackson, 1943, Chrysler Corporation Engineering Report No. 4904 (Unclassified).

46. SHEAR STRESS DISTRIBUTION ALONG GLUE LINE BETWEEN SKIN AND CAP STRIP OF AN AIRCRAFT WING by C. B. Norris and L. A. Ringelstetter, 1950, NACA Tech. Note 2152(Unclassified).

47. INVESTIGATION OF THE USE OF A RUBBER ANALOG IN THE STUDY OF STRESS DISTRIBUTION IN RIVETED AND CEMENTED JOINTS by L. R. Demarkles, 1955, NACA Tech. Note 3413 (Unclassified).

48. M. Reiner, RHEOLOGY, Encyclopedia of Physics, Vol. VI, Elasticity and Plasticity, Berlin, Springer-Verlag, 1958, pp. 434-436.

49. J. Stefan, S. B. AKAD, WISS, WIEN, Math. Naturw, Kl., Vol. 69, No. 713, p. 1874.

50. J. J. Bikerman, J. Coll. Sci., Vol. 2, 1947, p. 163.

51. W. H. Banks and C. C. Mill, TACKY ADHESION - A PRELIMINARY STUDY, J. Coll. Sci., Vol. 8, 1953, p. 137.

52. J. R. Scott, THEORY AND APPLICATION OF THE PARALLEL-PLATE PLASTIMETER, Trans. Inst. Rubber Ind., Vol. 7, 1931, p. 169.

53. R. L. Peek, PARALLEL PLATE PLASTOMETRY, Journal of Rheology, Vol. 3, 1932, p. 345.

54. H. Green, INDUSTRIAL RHEOLOGY AND RHEOLOGICAL STRUCTURES, New York, J. Wiley and Sons, 1949.

55. A. D. McLaren, T. T. Li, R. Rager, and H. Mark, THE MEANING OF TACH TEMPERATURE, Journal of Polymer Science, Vol. 7, 1951, p. 463.

56. L. R. G. Treloar, THE PHYSICS OF RUBBER ELASTICITY, Oxford, Clarendon Press, 1949.

57. J. Dow, ADHESION AND ADHESIVES, FUNDAMENTALS AND PRACTICE, Society of Chemical Industry, London, 1954.

58. A. Nadai, THEORY OF FLOW AND FRACTURE OF SOLIDS, New York, McGraw-Hill, 1951.

59. A. A. Griffith, THE PHENOMENA OF RUPTURE AND FLOW IN SOLIDS, Phil. Trans. Roy. Soc., Vol. 221, 1921, pp. 163-198.

60. G. R. Irwin, FRACTURE, Encyclopedia of Physics, Vol. XI, Elasticity and Plasticity, Berlin, Springer-Verlag, 1958, pp. 551-590.

61. University of Illinois, Urbana, Illinois, RELATIVELY UNEXPLORED ASPECTS OF FRACTURE MECHANICS by G. R. Irwin, October 1961, Summary of the Third of Three Series of Lectures Delivered in the Department of Theoretical and Applied Mechanics, University of Illinois (Unclassified).

62. J. R. Low, Jr., THE FRACTURE OF METALS, Progress in Materials Science, Vol. 12, No. 1, Pergamon Press, 1963, pp. 1-96.

63. FRACTURE, Proceedings of an International Conference on the Atomic Mechanisms of Fracture, Swampscott, Massachusetts, 12-16 April 1959, New York, John Wiley & Sons, Inc., 1959.

64. D. C. Drucker and J. J. Gilman, FRACTURE OF SOLIDS, Proceedings of an International Conference Sponsored by the Institute of Metals Division, American Institute of Mining, Metallurgical, and Petroleum Engineers, Maple Valley, Washington, 21-24 August 1962.

65. PREPRINT OF INTERNATIONAL CONFERENCE ON FRACTURE (1965), Organizing Committee of International Conference on Fracture, No. 3 (Chapters C, D, and E), Sendai, Japan, 12-17 September 1965.

66. B. Rosen, FRACTURE PROCESSES IN POLYMERIC SOLIDS; PHENOMENA AND THEORY, Interscience, New York, 1964.

67. P. Weiss, editor, ADHESION AND COHESION, Proceedings of the Symposium on Adhesion and Cohesion, General Motors Research Laboratories, Warren, Michigan, 1961, New York, Elsevier Publishing Company, 1962.

68. A THEORY OF ADHESIVE SCARF JOINTS WITH ANALYSIS OF TEST RESULTS by J. L. Lubkin, Phase I Report, U. S. Naval Ordnance Contract NOrd 13353 (Unclassified).

69. E. J. Ripling, S. Mostovoy, and R. L. Patrick, MEASURING FRACTURE TOUGHNESS OF ADHESIVE JOINTS, Materials Research and Standards, March 1964, pp. 129-134.

70. Materials Research Laboratory, Inc., FACTORS CONTROLLING THE STRENGTH OF COMPOSITE BODIES (INTERPHASE FRACTURING OF COMPOSITE BODIES) by E. J. Ripling and S. Mostovoy, 31 March 1965, Final Report to Bureau of Naval Weapons (Unclassified).

71. C. Fowlkes and I. Wolock, NRL, According to Reference (61) by G. Irwin.

72. FRACTURE TOUGHNESS TESTING AND ITS APPLICATION, Symposium Presented at the 67th Annual Meeting American Society for Testing and Materials, Chicago, Illinois, 21-26 June 1964.

73. FRACTURE TESTING OF HIGH STRENGTH SHEET MATERIALS: A REPORT OF A SPECIAL ASTM COMMITTEE, ASTM Bulletin, No. 243, June 1960, pp. 29-40; No. 244, February 1960, pp. 18-28; Materials Research and Standards, Vol. 1, No. 11, November 1961, pp. 877-885.

74. P. C. Paris and G. C. Sih, STRESS ANALYSIS OF CRACKS, Workshop in Fracture Mechanics, Denver, Colorado, 16-28 August 1964.

75. G. R. Irwin, FRACTURE MECHANICS, Structural Mechanics, Pergamon Press, 1960.

76. G. R. Irwin and J. A. Kies, CRITICAL ENERGY RATE ANALYSIS OF FRACTURE STRENGTH, Welding Journal Research Supplement, April 1954, pp. 193s-198s.

77. C. D. Beachem and R. M. N. Pelloux, ELECTRON FRACTOGRAPHY - A TOOL FOR THE STUDY OF MICRO MECHANISMS OF FRACTURING PROCESSES, Fracture Toughness Testing and Its Applications, Published by ASTM, 1961, pp. 210-246.

78. G. A. Ilkka and R. L. Scott, IMPACT TESTING OF ADHESIVE BONDS, Adhesion and Cohesion, Amsterdam, London, New York, Elsevier Publishing Company, 1962, pp. 65-73.

79. S. L. Reegan and G. A. Ilkka, THE ADHESION OF POLY-URETHANES TO METALS, Adhesion and Cohesion, Amsterdam, London, New York, Elsevier Publishing Company, 1962, pp. 159-175.

80. S. B. Newman and I. Wolock, MICROSCOPY OF COLOR PHENOMENA IN POLYMER FRACTURE, Adhesion and Cohesion, Amsterdam, London, New York, Elsevier Publishing Company, 1962, pp. 218-239.

81. R. F. Wegman and W. C. Tanner, STRENGTH OF EPOXY ADHESIVES WHEN STRESSED TO FAILURE IN MILLISECONDS, Adhesion, 1963, American Society for Testing and Materials, STP-360, 1963, pp. 163-176.

82. Picatinny Arsenal, Dover, New Jersey, RESPONSE OF EPOXY ADHESIVES WHEN STRESSED TO FAILURE IN MILLISECONDS by R. F. Wegman and E. L. O'Brien, June 1965, Technical Report 3122 (Unclassified).

83. Forest Products Laboratory, Madison, Wisconsin, STRENGTH PROPERTIES OF METAL-BONDING ADHESIVES AT TEMPER-ATURES FROM -100 F TO + 800 F by H. W. Eickner, July 1959, WADC-TR-59-152, RSIC 0017, Wright Air Development Center, Wright-Patterson Air Force Base, Ohio, Contract No. DA 33 (616)-58-1 (Unclassified).

84. R. C. Kausen, ADHESIVES FOR HIGH AND LOW TEMPERATURE, Paper Presented at the 7th National SAMPE Symposium, Los Angeles, California, 20-22 May 1964, RSIC 0375.

85. J. K. Kuno, COMPARISON OF ADHESIVE CLASSES FOR STRUCTURAL BONDING AT ULTRA-HIGH AND CRYOGENIC TEMPERATURE EXTREMES, Paper Presented at the 7th National SAMPE Symposium, Los Angeles, California, 20-22 May 1964, RSIC 0281.

86. George C. Marshall Space Flight Center, Huntsville, Alabama, ADHESIVE BONDING OF TITANIUM AND ITS ALLOYS by R. E. Keith, R. E. Monroe, and D. C. Martin, 4 August 1965, NASA Technical Memorandum TMX-53313 (Unclassified).

87. RESISTANCE OF ADHESIVE-BONDED METAL LAP JOINTS TO ENVIRONMENTAL EXPOSURE by W. Z. Olson, H. W. Eickner, and R. M. Lulling, October 1962, WADC TR 59-564, Pt. II (Unclassified).

88. L. H. Sharpe, ASPECTS OF THE PERMANENCE OF ADHESIVE JOINTS, Symposium on Structural Adhesives Bonding, Stevens Center, Hoboken, New Jersey, 14-16 September 1965.

89. R. E. Yeager, DEVELOPMENTS OF ADHESIVE SYSTEMS FOR EXTREME ENVIRONMENTS, Symposium on Structural Adhesives Bonding, Stevens Center, Hoboken, New Jersey, 14-16 September 1965.

90. N. A. DeBruyne, THE STRENGTH OF GLUED JOINTS, Aircraft Engineering, Vol. 16, 1944, p. 115.

91. M. L. Sheridan and H. R. Merriman, CONCLUSIONS DERIVED FROM EMPIRICAL STUDIES OF BONDED DETAILS FOR SANDWICH CONSTRUCTION, Second Pacific Area National Meeting, Los Angeles, California, ASTM Paper No. 83, September 1956.

92. H. Tombach, ADHESIVE JOINTS, Machine Design, Vol. 29, No. 7, 1957, pp. 113-120.

93. Boeing Aircraft Company, Wichita, Kansas, JOINT FACTORS OF METAL-BONDED JOINTS by D. Brown, 1960, A-3-4C (Unclassified).

94. A. Matting and K. Ulmer, UNTERSUCHUNGEN ZUM KLEBAN VON TITAN, Metal, Vol. 16, No. 6, 1962.

95. M. Levine, G. Ilkka, and P. Weiss, WETTABILITY OF SURFACE TREATED METALS AND THE EFFECT ON LAP SHEAR ADHESION, Adhesives Age, Vol. 7, No. 6, 1964, p. 24.

96. R. Houwink and G. Salmon, ADHESION AND ADHESIVES, VOL.I AND VOL. II, New York, Elsevier Publishing Company, 1965.

97. L. H. Sharpe and H. Schonhorn, CHLORTRIFLUORETHYLENE HOMOPOLYMERS AND COPOLYMERS, Journal of Polymer Science, B2, 1964, p. 719.

98. Forest Products Laboratory, U. S. Department of Agriculture, A STUDY OF METHODS FOR PREPARING 24S-T3 ALUMINUM ALLOY SHEET SURFACES FOR ADHESIVE BONDING, PART III by H. W. Eickner, 1950, Report No. 1813A (Unclassified).

99. Forest Products Laboratory, U. S. Department of Agriculture, ADHESIVE BONDING PROPERTIES OF VARIOUS METALS AS INFLUENCED BY THE CHEMICAL AND ANODIZING TREATMENTS OF THE SURFACES by H. W. Eickner, 1953, Report No. 1842 (Unclassified).

100. Forest Products Laboratory, U. S. Department of Agriculture, A STUDY OF METHODS FOR PREPARING 24S-T3 ALUMINUM ALLOY SHEET SURFACES FOR ADHESIVE BONDING by H. W. Eickner, and W. E. Schowalter, 1950, Report No. 1813 (Unclassified).

101. Chance Vaught Aircraft, BONDING OF MAGNESIUM ALLOY WITH REDUX ADHESIVE, 1951, Specification CVA 281.

102. Chance Vaught Aircraft, SURFACE TREATMENTS FOR MAGNESIUM ALLOYS, 1952, Specification CVA 40.

103. Chance Vaught Aircraft, METAL-TO-METAL BONDING OF MAGNESIUM ALLOY SHEET WITH REDUX ADHESIVES by H. W. Kleindienst, 1951, Report No. 7913 (Unclassified).

104. Chance Vaught Aircraft, ADHESIVE BONDING OF MAGNESIUM by A. Mellor, 1951, Structures Laboratory Test Report 21966.

105. ANODIC FILMS: CORROSION-PROTECTION FOR ALUMINUM ALLOYS, U. S. Army-Navy Aeronautical Specification AN-QQ-A-696a, 1941.

106. MAGNESIUM ALLOY: PROCESS FOR CORROSION PROTECTION, U. S. Military Specification MIL-M-3171, 1950.

107. SURFACE TREATMENTS (EXCEPT PRIMING AND PAINTING) FOR METAL AND METAL PARTS IN AIRCRAFT, U. S. Military Specification MIL-S-5002.

108. ANODIC OXIDATION TREATMENT FOR ALUMINUM AND ALUMINUM ALLOYS (CHROMIC ACID PROCESS), U. S. Navy Aeronautical Specification PT-19, 1940.

109. B. J. Aleck, THERMAL STRESSES IN A RECTANGULAR PLATE CLAMPED ALONG AN EDGE, J. Applied Mechanics, Vol. 16, 1949, pp. 118-122.

110. A. G. H. Dietz, H. Grinsfelder, and E. Reissner, ASME Transactions, Vol. 68, 1946, p. 238.

111. A. A. Wells, INFLUENCE OF RESIDUAL STRESS AND METALLURGICAL CHANGES ON LOW-STRESS BRITTLE FRACTURE IN WELDED STEEL PLATES, The Welding Journal, Vol. 40, No. 4, Research Supplement, April 1961, pp. 182s-192s.

112. H. Kihara, RECENT STUDIES IN JAPAN ON BRITTLE FRACTURE OF WELDED STEEL STRUCTURES UNDER LOW APPLIED STRESS, Document X-291-62 for Commission X of International Institute of Welding, 1962.

113. Redstone Scientific Information Center, U. S. Army Missile Command, Redstone Arsenal, Alabama, NONDESTRUCTIVE MEASUREMENT OF RESIDUAL STRESSES IN METALS AND METAL STRUCTURES by K. Masubuchi, April 1965, RSIC 410 (Unclassified).

114. A. A. Wells, THE BRITTLE FRACTURE STRENGTH OF WELDED STEEL PLATES, Quarterly Trans. Inst. Naval Arch., Vol. 48, No. 3, 1956, pp. 296-326.

115. H. Kihara and K. Masubuchi, EFFECT OF RESIDUAL STRESS ON BRITTLE FRACTURE, The Welding Journal, Vol. 38, No. 4, Research Supplement, 1959, pp. 159s-168s.

116. W. J. Hall, W. J. Nordell, and W. H. Munse, STUDIES OF WELDING PROCEDURES, The Welding Journal, Vol. 41, No. 11, Research Supplement, 1962, pp. 505s-518s.

117. W. J. Hall, J. R. Joshi, and W. H. Munse, STUDIES OF WELDING PROCEDURES-PHASE II, The Welding Journal, Vol. 44, No. 4, Research Supplement, 1965, pp. 182s-192s.

118. W. J. Hall and A. D. Chamberlain, STUDIES OF WELDING PROCEDURES - PHASE III, The Welding Journal, Vol. 45, No. 5, Research Supplement, 1966, pp. 193s-201s.

119. A. H. Cottrell, DISLOCATION AND PLASTIC FLOW IN CRYSTALS, London, Oxford University Press, 1953.

120. W. T. Read, DISLOCATIONS IN CRYSTALS, New York, McGraw-Hill, 1953.

121. J. B. Newkirk and J. H. Wernick, DIRECT OBSERVATIONS OF IMPERFECTIONS IN CRYSTALS, New York, Interscience, 1962.

122. D. R. Brame and T. Evans, DEFORMATIONS OF THIN FILMS ON SOLID SUBSTRATES, Philosophical Magazine, Series viii, Vol. 33, No. 3, 1958, pp. 971-986.

123. M. J. Marcinkowski and R. M. Fisher, MOVEMENT OF MISFIT DISLOCATION DURING DIFFUSION OF GOLD INTO COPPER-GOLD ALLOYS, Sixth International Congress for Electron Microscopy, Kyoto, Japan, 1966.

124. G. Dupouy, F. Perrier, and N. Takahashi, STUDY OF PRECIPITATES IN AL-25% ALLOY BY MEANS OF THE HIGH-VOLTAGE ELECTRON MICROSCOPE, Comptes Rendus, Vol. 256, 1963, p. 545.

125. P. Delavignette, J. Tournier, and S. Amelinckx, DIRECT OBSERVATION OF DISLOCATIONS DUE TO EPITAXY, Philosophical Magazine, Vol. 6, 1961, p. 1419.

126. J. W. Matthews, THE OBSERVATION OF DISLOCATIONS TO ACCOMODATE THE MISFIT BETWEEN CRYSTALS WITH DIFFERENT LATTICE PARAMETERS, Philosophical Magazine, Vol. 6, 1961, p. 1347.

127. J. C. Fisher, DISCUSSION, Trans. Amer. Inst. Min. (Metall) Engrs., Vol. 194, 1954, p. 531.

128. J. J. Gilman, ASTM STP No. 171, Philadelphia, Pennsylvania, 1955, pp. 3-13.

129. I. R. Kramer and L. J. Demer, EFFECTS OF ENVIRONMENT ON MECHANICAL PROPERTIES OF METALS, Progress in Materials Science, Vol. 9, 1961, pp. 133-199.

130. R. Roscoe, THE PLASTIC DEFORMATION OF CADMIUM SINGLE-CRYSTALS, Philosophical Magazine, Series 7, Vol. 21, 1936, p. 399.

131. A. F. Joffe, PHYSICS OF CRYSTALS, New York, McGraw-Hill, 1928.

132. J. Takamura, Mem. Fac. Eng. Kyoto University, Vol. 18, No. 3, 1956, pp. 255-279.

133. R. L. Fleischer and B. Chalmers, Trans. Met. Soc. Amer. Inst. Min. (Metall) Engrs., Vol. 212, No. 2, 1958, pp. 265-274.

134. A. K. Head, THE INTERACTION OF DISLOCATION AND BOUNDARIES, Philosophical Magazine, Vol. 44, 1953, p. 92.

135. M. J. Makin and E. N. Ca C. Andrade, Institute of Metals Monograph and Report Series No. 13, London, England, 1953, pp. 133-142.

136. H. Suzuki, S. Ikeda, and S. Takeuchi, Journal Phys. Soc., Japan, Vol. 11, 1946, p. 382.

137. F. D. Rosi, SURFACE EFFECTS OF PLASTIC PROPERTIES OF COPPER CRYSTALS, Acta Met., Vol. 5, 1957, pp. 348-350.

138. M. A. Adams, THE PLASTIC BEHAVIOR OF COPPER CRYSTALS CONTAINING ZINC IN THE SURFACE LAYER, Acta Met., Vol. 6, 1958, pp. 227-338.

139. J. Garstone, R. W. K. Honeycombe, and G. Greetham, EASY GLIDE OF CUBIC METAL CRYSTALS, Acta Met., Vol. 4, 1956, pp. 485-494.

140. B. Chalmers and R. S. Davis, Conference of Dislocations Mech. Properties Crystals, Lake Placid, New York, 1956, New York, John Wiley, 1957, pp. 232-233.

141. E. D. Sweetland and E. R. Parker, EFFECT OF SURFACE CONDITION OF CREEP OF SOME COMMERCIAL METALS, Journal of Applied Science, Vol. 20, 1953, pp. 30-32.

142. A. W. Cochardt, ABNORMAL AFTER-EFFECT OF TWISTED METAL WIRES UPON HEATING, Acta Met., Vol. 3, 1955, pp. 607-608.

143. W. A. Jemian and C. C. Law, DISCUSSION OF THE EFFECTS OF METALLIC COATINGS ON THE TORSIONAL RECOVERY OF WIRES, to be Published in Acta Metallurgica.

144. J. Kramer, Z. Physik, Vol. 125, 1949, p. 739.

145. J. Kramer, Z. Physik, Vol. 128, 1950, p. 538.

146. V. I. Lichtman, P. A. Rehbinder, and G. V. Karpenko, EFFECT OF A SURFACE ACTIVE MEDIUM ON THE DEFORMATION OF METALS, London, Her Majesty's Stationary Office, 1958.

147. M. Metzger and T. A. Read, THE EFFECT OF SURFACE FILMS ON THE CREEP OF CADMIUM CRYSTALS, Transactions of the Metallurgical Society of AIME, Vol. 2, No. 212, 1958, pp. 236-243.

DISTRIBUTION

EXTERNAL	No. of Copies
Air University Library ATTN: AUL3T Maxwell Air Force Base, Alabama 36112	1
U. S. Army Electronics Proving Ground ATTN: Technical Library Fort Huachuca, Arizona 85613	1
U. S. Naval Ordnance Test Station ATTN: Technical Library, Code 753 China Lake, California 93555	1
U. S. Naval Ordnance Laboratory ATTN: Library Corona, California 91720	1
Lawrence Radiation Laboratory ATTN: Technical Information Division P. O. Box 808 Livermore, California 94550	1
Sandia Corporation ATTN: Technical Library P. O. Box 969 Livermore, California 94551	1
U. S. Naval Postgraduate School ATTN: Library Monterey, California 93940	1
Electronic Warfare Laboratory, USAECOM Post Office Box 205 Mountain View, California 94042	1
Jet Propulsion Laboratory ATTN: Library (TDS) 4800 Oak Grove Drive Pasadena, California 91103	2
U. S. Naval Missile Center ATTN: Technical Library, Code N3022 Point Mugu, California 93041	1
U. S. Army Air Defense Command ATTN: ADSX Ent Air Force Base, Colorado 80912	1
Central Intelligence Agency ATTN: OCR/DD-Standard Distribution Washington, D. C. 20505	4
Harry Diamond Laboratories ATTN: Library Washington, D. C. 20438	1
Scientific & Tech. Information Div., NASA ATTN: ATS Washington, D. C. 20546	1

	No. of Copies
U. S. Atomic Energy Commission ATTN: Reports Library, Room G-017 Washington, D. C. 20545	1
U. S. Naval Research Laboratory ATTN: Code 2027 Washington, D. C. 20390	1
Weapons Systems Evaluation Group Washington, D. C. 20305	1
John F. Kennedy Space Center, NASA ATTN: KSC Library, Documents Section Kennedy Space Center, Florida 32899	2
APGC (PGBPS-12) Eglin Air Force Base, Florida 32542	1
U. S. Army CDC Infantry Agency Fort Benning, Georgia 31905	1
Argonne National Laboratory ATTN: Report Section 9700 South Cass Avenue Argonne, Illinois 60440	1
U. S. Army Weapons Command ATTN: AMSWE-RDR Rock Island, Illinois 61201	1
Rock Island Arsenal ATTN: SWERI-RDI Rock Island, Illinois 61201	1
U. S. Army Cmd. & General Staff College ATTN: Acquisitions, Library Division Fort Leavenworth, Kansas 66027	1
Combined Arms Group, USACDC ATTN: Op. Res., P and P Div. Fort Leavenworth, Kansas 66027	1
U. S. Army CDC Armor Agency Fort Knox, Kentucky 40121	1
Michoud Assembly Facility, NASA ATTN: Library, I-MICH-OSD P. O. Box 29300 New Orleans, Louisiana 70129	1
Aberdeen Proving Ground ATTN: Technical Library, Bldg. 313 Aberdeen Proving Ground, Maryland 21005	1
NASA Sci. & Tech. Information Facility ATTN: Acquisitions Branch (S-AK/DL) P. O. Box 33 College Park, Maryland 20740	5
U. S. Army Edgewood Arsenal ATTN: Librarian, Tech. Info. Div. Edgewood Arsenal, Maryland 21010	1

	No. of Copies
National Security Agency ATTN: C3/TDL Fort Meade, Maryland 20755	1
Goddard Space Flight Center, NASA ATTN: Library, Documents Section Greenbelt, Maryland 20771	1
U. S. Naval Propellant Plant ATTN: Technical Library Indian Head, Maryland 20640	1
U. S. Naval Ordnance Laboratory ATTN: Librarian, Eva Liberman Silver Spring, Maryland 20910	1
Air Force Cambridge Research Labs. L. G. Hanscom Field ATTN: CRMXLR/Stop 29 Bedford, Massachusetts 01730	1
Springfield Armory ATTN: SWESP-RE Springfield, Massachusetts 01101	1
U. S. Army Materials Research Agency ATTN: AMXMR-ATL Watertown, Massachusetts 02172	1
Strategic Air Command (OAI) Offutt Air Force Base, Nebraska 68113	1
Picatinny Arsenal, USAMUCOM ATTN: SMUPA-VA6 Dover, New Jersey 07801	1
U. S. Army Electronics Command ATTN: AMSEL-CB Fort Monmouth, New Jersey 07703	1
Sandia Corporation ATTN: Technical Library P. O. Box 5800 Albuquerque, New Mexico 87115	1
ORA(RRRT) Holloman Air Force Base, New Mexico 88330	1
Los Alamos Scientific Laboratory ATTN: Report Library P. O. Box 1663 Los Alamos, New Mexico 87544	1
White Sands Missile Range ATTN: Technical Library White Sands, New Mexico 88002	1
Rome Air Development Center (EMLAL-1) ATTN: Documents Library Griffiss Air Force Base, New York 13440	1

	No. of Copies
Brookhaven National Laboratory Technical Information Division ATTN: Classified Documents Group Upton, Long Island, New York 11973	1
Watervliet Arsenal ATTN: SWEWV-RD Watervliet, New York 12189	1
U. S. Army Research Office (ARO-D) ATTN: CRD-AA-IP Box CM, Duke Station Durham, North Carolina 27706	1
Lewis Research Center, NASA ATTN: Library 21000 Brookpark Road Cleveland, Ohio 44135	1
Systems Engineering Group (RTD) ATTN: SEPIR Wright-Patterson Air Force Base, Ohio 45433	1
U. S. Army Artillery & Missile School ATTN: Guided Missile Department Fort Sill, Oklahoma 73503	1
U. S. Army CDC Artillery Agency ATTN: Library Fort Sill, Oklahoma 73504	1
U. S. Army War College ATTN: Library Carlisle Barracks, Pennsylvania 17013	1
U. S. Naval Air Development Center ATTN: Technical Library Johnsville, Warminster, Pennsylvania 18974	1
Frankford Arsenal ATTN: C-2500-Library Philadelphia, Pennsylvania 19137	1
Div. of Technical Information Ext., USAEC P. O. Box 62 Oak Ridge, Tennessee 37830	1
Oak Ridge National Laboratory ATTN: Central Files P. O. Box X Oak Ridge, Tennessee 37830	1
Air Defense Agency, USACDC ATTN: Library Fort Bliss, Texas 79916	1
U. S. Army Air Defense School ATTN: AKBAAS-DR-R Fort Bliss, Texas 79906	1

	No. of Copies
U. S. Army CDC Nuclear Group Fort Bliss, Texas 79916	1
Manned Spacecraft Center, NASA ATTN: Technical Library, Code BM6 Houston, Texas 77058	1
Defense Documentation Center Cameron Station Alexandria, Virginia 22314	20
U. S. Army Research Office ATTN: STINFO Division 3045 Columbia Pike Arlington, Virginia 22204	1
U. S. Naval Weapons Laboratory ATTN: Technical Library Dahlgren, Virginia 22448	1
U. S. Army Engineer Res. & Dev. Labs. ATTN: Scientific & Technical Info. Br. Fort Belvoir, Virginia 22060	2
Langley Research Center, NASA ATTN: Library, MS-185 Hampton, Virginia 23365	1
Research Analysis Corporation ATTN: Library McLean, Virginia 22101	1
U. S. Army Tank Automotive Center ATTN: SMOTA-RTS.1 Warren, Michigan 48090	1
Hughes Aircraft Company Electronic Properties Information Center Florence Ave. & Teale St. Culver City, California 90230	1
Atomics International, Div. of NAA Liquid Metals Information Center P. O. Box 309 Canoga Park, California 91305	1
Battelle Memorial Institute ATTN: Mr. Vern Ellzey 505 King Avenue Columbus, Ohio 43201	25

INTERNAL

	No. of Copies
Headquarters U. S. Army Missile Command Redstone Arsenal, Alabama	
ATTN: AMSMI-D	1
AMSMI-XE, Mr. Lowers	1
AMSMI-XS, Dr. Carter	1
AMSMI-Y	1
AMSMI-R, Mr. McDaniel	1
AMSMI-RAP	1
AMSMI-RBLD	10
USACDC-LnO	1
AMSMI-RB, Mr. Croxton	1
AMSMI-RBR	25
AMSMI-R, Mr. Fagan	1
AMSMI-RR, Dr. Hallowes	1
AMCPM-NX, Dr. Lange	1
AMSMI-RDP	1
AMSMI-RKF	1
AMSMI-RLH	1
AMSMI-RLC	1
AMSMI-RSM, Mr. Wheelahan	10
National Aeronautics & Space Administration Marshall Space Flight Center Huntsville, Alabama	
ATTN: MS-T, Mr. Wiggins	5
DIR, Mr. Shepherd	1
R-RP-N, Dr. Shelton	1
I-PL-CH, Mr. Goodrum	1
R-ME-MM, Mr. Wilson	2
R-ME-DF	1
R-P&VE-M	1
R-P&VE-S	1
R-ASTR-M	1
R-TEST-BD	1

UNCLASSIFIED
Security Classification

DOCUMENT CONTROL DATA - R&D		
(Security classification of title, body of abstract and indexing annotation must be entered when the overall report is classified)		
1. ORIGINATING ACTIVITY *(Corporate author)* Battelle Memorial Institute, 505 King Avenue, Columbus, Ohio 43201	2a. REPORT SECURITY CLASSIFICATION: Unclassified 2b. GROUP: N/A	
3. REPORT TITLE: FUNDAMENTALS OF SELECTED ASPECTS OF DEFORMATION CHARACTERISTICS OF ADHESIVE-BONDED JOINTS AND METAL-ADHESIVE INTERFACES		
4. DESCRIPTIVE NOTES *(Type of report and inclusive dates)*: State-of-the-art survey		
5. AUTHOR(S) *(Last name, first name, initial)*: Masubuchi, Koichi and Keith, R. E.		
6. REPORT DATE: 27 January 1967	7a. TOTAL NO. OF PAGES: 97	7b. NO. OF REFS: 147
8a. CONTRACT OR GRANT NO. b. PROJECT NO. (DA) c. 01-021-AMC-14693(Z) d.	9a. ORIGINATOR'S REPORT NUMBER(S): RSIC-642 9b. OTHER REPORT NO(S) *(Any other numbers that may be assigned this report)*: AD	
10. AVAILABILITY/LIMITATION NOTICES: Distribution of this document is unlimited.		
11. SUPPLEMENTARY NOTES: None	12. SPONSORING MILITARY ACTIVITY: Redstone Scientific Information Center, Research and Development Directorate, U. S. Army Missile Command, Redstone Arsenal, Alabama 35809	

13. ABSTRACT

This report presents a state-of-the-art survey on selected aspects of fundamentals of deformation characteristics of adhesive-bonded joints and metal-adhesive interfaces.

The report is divided into three separate parts:

Chapter 1: Fundamentals of Deformation and Fracture of Adhesive-Bonded Joints.
Chapter 2: Mechanisms of Deformation of Metal-Adhesive Interfaces.
Chapter 3: Conclusions and Recommendations.

Chapter 1 covers the following subjects:

1) Theoretical analyses of elastic stress distribution in adhesive-bonded joints.
2) Experimental stress analyses of adhesive-bonded joints.
3) Rheology of adhesive-bonded joints.
4) Fracture of adhesive-bonded joints.

(Continued on page 100)

UNCLASSIFIED
Security Classification

14. KEY WORDS	LINK A		LINK B		LINK C	
	ROLE	WT	ROLE	WT	ROLE	WT
Adhesive-bonded joints						
Metal joint deformation						
Joint stress analysis						
Adhesive joint fracture						
Joint design						
Metal structures						

INSTRUCTIONS

1. ORIGINATING ACTIVITY: Enter the name and address of the contractor, subcontractor, grantee, Department of Defense activity or other organization *(corporate author)* issuing the report.

2a. REPORT SECURITY CLASSIFICATION: Enter the overall security classification of the report. Indicate whether "Restricted Data" is included. Marking is to be in accordance with appropriate security regulations.

2b. GROUP: Automatic downgrading is specified in DoD Directive 5200.10 and Armed Forces Industrial Manual. Enter the group number. Also, when applicable, show that optional markings have been used for Group 3 and Group 4 as authorized.

3. REPORT TITLE: Enter the complete report title in all capital letters. Titles in all cases should be unclassified. If a meaningful title cannot be selected without classification, show title classification in all capitals in parenthesis immediately following the title.

4. DESCRIPTIVE NOTES: If appropriate, enter the type of report, e.g., interim, progress, summary, annual, or final. Give the inclusive dates when a specific reporting period is covered.

5. AUTHOR(S): Enter the name(s) of author(s) as shown on or in the report. Enter last name, first name, middle initial. If military, show rank and branch of service. The name of the principal author is an absolute minimum requirement.

6. REPORT DATE: Enter the date of the report as day, month, year; or month, year. If more than one date appears on the report, use date of publication.

7a. TOTAL NUMBER OF PAGES: The total page count should follow normal pagination procedures, i.e., enter the number of pages containing information.

7b. NUMBER OF REFERENCES: Enter the total number of references cited in the report.

8a. CONTRACT OR GRANT NUMBER: If appropriate, enter the applicable number of the contract or grant under which the report was written.

8b, 8c, & 8d. PROJECT NUMBER: Enter the appropriate military department identification, such as project number, subproject number, system numbers, task number, etc.

9a. ORIGINATOR'S REPORT NUMBER(S): Enter the official report number by which the document will be identified and controlled by the originating activity. This number must be unique to this report.

9b. OTHER REPORT NUMBER(S): If the report has been assigned any other report numbers *(either by the originator or by the sponsor)*, also enter this number(s).

10. AVAILABILITY/LIMITATION NOTICES: Enter any limitations on further dissemination of the report, other than those imposed by security classification, using standard statements such as:

(1) "Qualified requesters may obtain copies of this report from DDC."

(2) "Foreign announcement and dissemination of this report by DDC is not authorized."

(3) "U. S. Government agencies may obtain copies of this report directly from DDC. Other qualified DDC users shall request through
____________________________."

(4) "U. S. military agencies may obtain copies of this report directly from DDC. Other qualified users shall request through
____________________________."

(5) "All distribution of this report is controlled. Qualified DDC users shall request through
____________________________."

If the report has been furnished to the Office of Technical Services, Department of Commerce, for sale to the public, indicate this fact and enter the price, if known.

11. SUPPLEMENTARY NOTES: Use for additional explanatory notes.

12. SPONSORING MILITARY ACTIVITY: Enter the name of the departmental project office or laboratory sponsoring *(paying for)* the research and development. Include address.

13. ABSTRACT: Enter an abstract giving a brief and factual summary of the document indicative of the report, even though it may also appear elsewhere in the body of the technical report. If additional space is required, a continuation sheet shall be attached.

It is highly desirable that the abstract of classified reports be unclassified. Each paragraph of the abstract shall end with an indication of the military security classification of the information in the paragraph, represented as *(TS), (S), (C), or (U)*.

There is no limitation on the length of the abstract. However, the suggested length is from 150 to 225 words.

14. KEY WORDS: Key words are technically meaningful terms or short phrases that characterize a report and may be used as index entries for cataloging the report. Key words must be selected so that no security classification is required. Identifiers, such as equipment model designation, trade name, military project code name, geographic location, may be used as key words but will be followed by an indication of technical context. The assignment of links, rules, and weights is optional.

DD Form 1473 (concluded)

5) Effects of loading and environmental conditions on deformation and fracture of adhesive-bonded joints.
6) Design and fabrication problems.

Chapter 2 discusses atomistic mechanisms of deformation of metal-adhesive interfaces.

Chapter 3 presents the conclusions derived from findings of the survey. Also, on the basis of findings observed during this survey, recommendations are given for future research for better understanding of the fundamentals of deformation and fracture of adhesive-bonded joints.

The report was written for the specific purpose of assisting another investigation in the field of adhesive-bonded joints. Therefore, it has somewhat narrow objectives. The report is not intended to be a comprehensive treatment of the subject of adhesive-bonded joints.